

Spectroscopy of free radicals and radical containing entrance-channel complexes in superfluid helium nano-droplets

Jochen Küpper*

Fritz-Haber-Institut der MPG, Faradayweg 4-6, 14195 Berlin, Germany

Jeremy M. Merritt[§]

*University of North Carolina, Chapel Hill, NC 27599, USA and
Fritz-Haber-Institut der MPG, Faradayweg 4-6, 14195 Berlin, Germany*

Dedicated to Roger E. Miller[†]

(Dated: 20th August 2018)

The spectroscopy of free radicals and radical containing entrance-channel complexes embedded in superfluid helium nano-droplets is reviewed. The collection of dopants inside individual droplets in the beam represents a micro-canonical ensemble, and as such each droplet may be considered an isolated cryo-reactor. The unique properties of the droplets, namely their low temperature (0.4 K) and fast cooling rates ($\sim 10^{16}$ K s⁻¹) provides novel opportunities for the formation and high-resolution studies of molecular complexes containing one or more free radicals. The production methods of radicals are discussed in light of their applicability for embedding the radicals in helium droplets. The spectroscopic studies performed to date on molecular radicals and on entrance / exit-channel complexes of radicals with stable molecules are detailed. The observed complexes provide new information on the potential energy surfaces of several fundamental chemical reactions and on the intermolecular interactions present in open-shell systems. Prospects of further experiments of radicals embedded in helium droplets are discussed, especially the possibilities to prepare and study high-energy structures and their controlled manipulation, as well as the possibility of fundamental physics experiments.

PACS numbers: 33.15.-e,34.20.-b,39.10.+j,82.30.Cf,82.33.Fg

Keywords: free radicals; superfluid helium nano-droplets; infrared spectroscopy; entrance / exit-channel complexes; reaction dynamics; high energy structures; chemical energy storage

*Author to whom correspondence should be addressed; electronic address: jochen@fhi-berlin.mpg.de

†Deceased 6. November 2005

[§]Electronic address: merritjm@unc.edu

Contents

I. Introduction	3
II. Experimental methods	4
A. Spectroscopy in superfluid helium nano-droplets	4
B. Radical production	5
Pyrolysis	6
Other schemes	6
III. Radical monomers in helium droplets	7
A. Propargyl	7
B. Nitric oxide	7
C. Other species	8
IV. Radical-containing molecular complexes	8
A. Complexes containing halogen atoms	9
B. Complexes of hydrocarbon radicals	13
1. Complexes of methyl radical with HF and HCN	13
2. Larger hydrocarbon radicals	14
C. NO-HF	15
V. Interactions between helium droplets and embedded molecules	16
VI. Future directions	17
A. High energy structures for chemical energy storage	17
B. Other applications	20
C. Experimental improvements	20
VII. Summary	21
Acknowledgments	21
References	21

I. INTRODUCTION

Doped superfluid helium nano-droplets have emerged as a new and exciting tool for the study of the structure and dynamics of a quantum solvent as well as the embedded or attached atomic and molecular impurities themselves. The unique properties of the droplets, namely their low temperature and rapid cooling, make them a versatile tool for spectroscopic studies of metastable species. Although there have been a number of reviews on the spectroscopy of particles embedded in or attached to helium nano-droplets [1–7], none of these articles covers the recent advances made in the study of open shell, free radical metastable species. Therefore, an overview of this emerging field and the new possibilities it provides for the understanding of chemical reaction dynamics is timely.

Radicals and molecular ions are among the most chemically reactive species known and play a key role in chemistry ranging from combustion processes [8] to the upper atmosphere [9] and molecular synthesis in the interstellar medium [10]. This high reactivity comes at a considerable cost to experimentalists; such transient species are often very difficult to maintain at sufficient concentrations to be probed experimentally. While a great deal of progress has been made by isolating radicals in vacuum, much less is known about the interactions of radicals, or more generally, the features of their potential energy surfaces (PES). A focal point in chemical reaction dynamics has been to elucidate the properties of the transition state, the point on the PES where bonds are broken and reformed. Already in 1884 van't Hoff proposed [11], and five years later Arrhenius provided an physical interpretation [12], for an empirical, analytical expression for the rate constant of a reaction, relating it to an energy penalty needed to produce an *activated complex*, which could then go on to produce the products. A quantum-mechanical interpretation of the activation process was first given by London [13] and successively by Eyring and Polanyi [14], who introduced the concepts of a reaction path and the transition state as a saddle-point on a multi-dimensional PES (*Sattelgebiet des „Resonanzgebirges“*) for the $H+H_2$, $H+HBr$, and $H+Br_2$ reaction systems.[245] Later, the efficiency of a reaction could be predicted based on the initial reagent energy (whether it be translational or vibrational) by developing the concept of early or late potential barriers [15, 16]. Recent advances in reactive scattering have now enabled fully (initial and final) quantum state resolved reaction crosssections to be determined for a few prototype systems, like $F+H_2$ [17–20], which was once considered to be the *holy grail* of the field. The matrix of initial and final quantum states provides a rigorous test of theoretical potential energy surfaces. One should note, however, that even at the full state to state level, impact parameter averaging acts to convolute the experimental results, sometimes making it difficult to draw quantitative conclusions on the detailed features of the potential. Furthermore,

the scalability of such experiments to larger and larger systems is prohibitive. Oriented collisions [21–24], and especially the application of state-selected, decelerated molecular beams [25–29] and their use in scattering experiments [30] are likely to be important tools enabling the experimentalist to further reduce the effects of impact parameter averaging.

While reactive scattering is a sensitive probe of the repulsive wall of the PES, much less is known about the long-range dispersive forces between reactive species. Indeed, already Eyring and Polanyi [14] discussed the additional effects of dispersion forces on the PES, which predicted a minimum for the symmetric H_3 molecule on their collinear PES. For the heavier systems they concluded that their calculations were not accurate enough to incorporate these effects quantitatively. However, the van der Waals minima which result from the balance of attractive and repulsive forces lie at the base of the transition state, and correspond to weakly bound clusters of two (or more) reactants or products. These species are labeled as entrance or exit channel complexes, respectively. Given that the barriers to chemical reaction are typically several orders of magnitude larger than dispersion (van der Waals) forces, the importance of these van der Waals forces to reaction dynamics has largely been neglected. Recent experimental and theoretical work on the $Cl+HD \rightarrow HCl(DCl)+H(D)$ reaction, however, has shown that the corresponding orientational effects of the long range potential can strongly influence the branching ratios and the final state distributions by giving the reactants a torque, towards or away from the transition state [31–35]. Therefore, the long-range van der Waals forces can no longer be neglected for obtaining really quantitative results. For collisions at even lower temperature [30] such effects will be even more important. Moreover, also for the dissociation of formaldehyde [36, 37] and the hydrogen abstraction from hydrocarbon molecules by chlorine [38] the effects of long-range van der Waals interactions have clearly been observed. Therefore, it must be concluded, that a quantitative understanding of van der Waals wells of molecular complexes is imperative.

One of the legacies that Roger E. Miller has left with us is the sensitivity of high resolution spectroscopy of such weakly bound complexes as a probe of the surrounding PES. Here again, theory plays a crucial role in solving the multidimensional problem standing between the PES and the observed spectral transitions between eigenstates of the exact Hamiltonian. More recently, these spectroscopic techniques have been applied to reactive systems, where now the experimental methods have the added challenge of stabilizing the weakly bound complex and preventing the reaction. Sometimes the cooling provided by a free jet expansion is sufficient to stabilize such pre-reactive species, which can then be studied spectroscopically. The most common examples are $X-HY$ radicals, where X are, for example, H_2 or noble gas atoms and $Y=C, O, N, S, B$, or CN radicals. Many of

the previous experiments have been performed using an noble-gas atom such as argon or neon to study the effects of polarization, and in these cases no reaction can occur [39, 40]. Complexes have also been observed between reactive partners such as, for example, OH+CO [41], OH+H₂ [42–46], and CN+H₂ [47–50]. However, in these systems the barriers to reaction are still quite large. So far these experimental techniques have relied on the exquisite sensitivity of laser induced fluorescence double-resonance methods in order to measure the spectra, somewhat limiting the choice of chromophores.

Many transient radicals have also been studied in solid noble-gas matrices [51–53]. Indeed, the inert matrix can be used to keep the radicals from interacting with one another, and in general the number of radicals can be built up using long deposition times. One can also raise the temperature of the solid matrix, which gives the dopants some mobility, eventually initiating the reactions. Due to the large matrix effects, however, the spectra are often strongly perturbed, thus limiting the amount of information which can be extracted. Indeed, the highly anisotropic interaction is found to quench the free rotation of most molecules. In contrast to the more classical cryogenic matrices described above, cold, solid para-hydrogen matrices have also recently been used to study molecules in a more soft, quantum mechanical matrix [54–56], but even this special matrix does not give such great control over the growth process as liquid helium droplets. Reactions of embedded impurities with H₂, the matrix material itself, can easily be studied, but for other purposes the matrix is not as inert as noble-gas environments [57].

Liquid helium nano-droplets combine the advantages of both types of solid matrix environments. They are inert due to the very noble, unreactive character of the helium atoms constituting the matrix and they perturb embedded impurities only very weakly due to their quantum-fluid nature, which manifests itself in the superfluidity of the droplets [58]. The droplets provide a very low ambient temperature of approximately 0.37 K, due to evaporative cooling and the low binding energy of helium atoms to the droplet. Molecules embedded in ⁴He droplets show free rotation [59]. The formation of weakly bound molecular complexes inside helium nano-droplets proceeds through unique growth dynamics which are mainly determined by long-range forces between the complexation partners [1]. Therefore, often metastable clusters are stabilized and can be studied in the droplets [60, 61]. Additional information on the PES can be obtained using infrared-infrared double-resonance spectroscopy, where the photo-initiated annealing of complexes provides branching ratios between different minima and limits on the barrier heights and allows to observe the products of photo-initiated chemical reactions [62, 63].

Extending such studies to transient, reactive species can provide novel materials, that can be studied using high-

resolution spectroscopy. It should be possible, for example, to build linear chains from polar OH radicals just like in the case of HCN molecules [60], or similar highly reactive systems. Such systems are ideal candidates for chemical energy storage and provide large energy-to-mass ratios. The details of such prospective experiments are discussed in section VIA. Moreover, the spectroscopic study of such highly energetic systems provides complementary information to scattering experiments on chemical reaction dynamics.

In this review we will detail the experimental methods for embedding and studying radicals embedded in superfluid helium nano-droplets. In the following section a general introduction into helium droplet experiments is given, followed by the details of radical production. Then we will describe the experiments on radical monomers (section III) and on radical-molecule van der Waals complexes in section IV. Afterward, a discussion of molecule-droplet interactions, emphasizing the additional information from spectroscopy of open-shell systems embedded in helium droplets (section V), and an outlook for further applications (section VI) are given.

II. EXPERIMENTAL METHODS

A. Spectroscopy in superfluid helium nano-droplets

The experimental details concerning the production of neat and doped helium droplets have been given in previous reviews [1–6] and their thermodynamic properties have been discussed [64–66]. Therefore, here we will only discuss the relevant details and specialties for embedding radicals in the droplets. A schematic of the first apparatus for infrared spectroscopy of radicals embedded in helium droplets [67], built at the University of North Carolina at Chapel Hill (UNC), is shown in Figure 1. In brief, the setup consists of a continuous helium droplet beam source and several, differentially pumped vacuum chambers. The source chamber contains the supersonic droplet beam source. The droplet beam passes through a skimmer into a region with a series of load

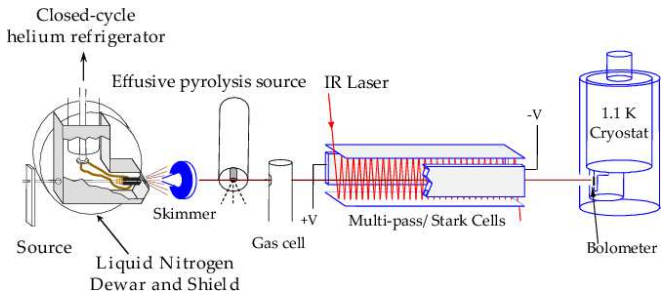


Figure 1: Experimental setup for the infrared spectroscopy of radicals in superfluid helium droplets; see text for details.

lock ports to introduce pick-up sources of varying nature. After the droplets are doped they fly into a laser excitation region, where a multipass cell, consisting of two plane, parallel gold-coated mirrors, is used to increase the laser-droplet beam interaction. This spectroscopy region also has a pair of parallel electrodes, providing homogeneous fields up to 80 kV/cm, in which Stark and pendular spectroscopy [68] can be performed. In all experiments reported here, the electric field is parallel to the laser-polarization, yielding $\Delta m = 0$ selection rules for the associated Stark and pendular spectra. The overall kinetic energy of the beam is then detected further downstream by a cooled semiconductor bolometer detector [1]. Alternatively, mass-spectrometric detection has been used in similar ways [1, 2], however, in that case the infrared laser beam is typically sent collinear to the droplet beam to achieve sufficient signal to noise ratios.

Droplets are typically produced by expanding high-pressure helium (20–100 bar) through a small, cooled pinhole (5–10 μm , 5–30 K), as originally demonstrated by Becker *et al.* in 1961 [69]. Droplets are formed in the early, high-pressure portion of the expansion and then successively cooled by evaporation. In the case of ^4He , as used in all spectroscopic studies on radicals embedded in helium droplets so far, the evaporation temperature converges at ~ 0.37 K [64] and ^4He droplets exhibit superfluidity under these conditions [58].

Atomic and molecular *impurities* are embedded in the droplets by pick-up in scattering regions [1, 2]. The pick-up process is sequential, that is, individual atoms and molecules are picked up from the scattering gas, where only low densities are necessary, because the pick-up probability is determined by the large, geometrical cross-sections of the droplets. The cooling of dopants inside the helium droplet occurs on a timescale considerably faster than the complexation of multiple embedded species. For $(\text{HCN})_n$ complexes embedded in a single droplet, for example, about 1000 cm^{-1} binding energy are released upon addition of an additional HCN molecule. If that energy would be deposited in the molecular complex, the cluster would anneal to its global minimum structure. However, the helium removes the energy quickly as the complex is forming, forcing it to stay at the zero-point level while traversing the PES. Therefore, the complexes are often trapped in local minima and metastable species can be observed [60, 61]. Moreover, since the pick-up can be performed in multiple separate scattering regions, considerable control over the formation of larger clusters can be achieved, as, for example, shown for HF- Ar_n complexes [70]. This separable pick-up also allows to produce clusters with quite complex compositions, possibly containing multiple species, and to embed species under quite different conditions into the droplet. For example, thermally labile bio-molecules and metal atoms from a hot oven or radicals from an 1800 K pyrolysis source can be embedded in the same droplet, because the two species only come together in the cold confines of the

droplet. This unique production process allows to specifically design desired complexes inside helium droplets.

All molecular radicals or radical-molecule complexes embedded in a helium droplet that have been studied using high-resolution spectroscopy so far have either been stable molecules, like NO, that were picked up in an ordinary scattering chamber, or were produced in a continuous effusive pyrolysis source developed some years ago [67]; see section II B for details.

Different detection schemes used in helium droplet spectroscopy have been described before [1, 2]. In all studies described in detail in this review, infrared depletion spectroscopy is used, where the evaporation of helium atoms from the droplet due to resonant infrared excitation of the dopant is detected [1]. In most of the studies reported here the reduced total kinetic energy of the droplet beam on a 1.1 K bolometer is measured using lock-in techniques, but mass spectrometric techniques, albeit less sensitive, have also been employed [1], also for performing electronic spectroscopy of doped helium droplets [2, 7]. However, the bolometer detection proved to be the most sensitive so far. It is very general as it detects directly the evaporation of helium atoms from the droplet and does not require any specialized UV laser systems. Due to its quasi-continuous operation mode it matches the continuous droplet beams very well and provides optimal experimental duty cycle.

In the interpretation of rotationally resolved spectra of species embedded in helium droplets the *matrix effects* of the droplet environment needs to be considered. Vibrational frequencies of the embedded molecules are typically shifted very little from their gas-phase values, and due to the superfluidity of the droplets, free rotation of the embedded species can be observed [59]. The obtained rotational constants, however, are reduced from their corresponding gas-phase values [1, 59] and the influence of the droplet environment on the electronic structure can also be considerable. These effects are discussed in section V.

B. Radical production

Some molecular radicals are not transient at all and can be bought and stored under ambient conditions. Therefore a simple pick-up cell can be used to embed these species in the droplets. NO is an example of such a molecule that has also been studied in helium droplets [71].

For transient species, however, one has to resort to *in situ* production of the radical in the experiment. Several different methods for producing radicals for molecular beam studies have been developed, including pyrolysis, radio-frequency or microwave discharges, corona discharges, and photolysis [72, 73]. The most popular sources for

use in combination with the extreme cooling provided in supersonic jet experiments are flash pyrolysis [74–76], electric discharge sources [77–79], and photolysis sources [80–82].

These methods are, however, not currently generally applicable for embedding molecules into helium droplets, as they are mostly operated in a pulsed fashion and require relatively high gas-pressure. While these radical sources are efficient in producing a large number of radicals, especially the discharge and photolysis sources often produce a large number of by-products. For gas-phase studies this does not necessarily represent a problem as long as the background pressure is kept low enough to prevent collisions, and that the target-radical concentration is high enough for the experimental sensitivity. Also, if a precursor or decomposition product absorbs in the same spectral region as the species of interest, then it may be difficult to separate out the overlapping bands. In a helium droplet experiment, however, all species are picked up by the droplets without any discrimination. Therefore, extremely clean sources of radicals are required for these experiments in order not to contaminate all droplets. This includes buffer gas, which makes up most of the gas-phase expansion. Moreover, most helium droplet experiments today are operated as continuous beams and are therefore most efficiently used with continuous doping methods. Coupling pulsed radical sources to these beams, especially photolysis sources using intense pulsed lasers operating at 10 Hz, leads to large reductions of duty cycle and correspondingly lower signals. Once pulsed helium droplet sources are wider applicable [83, 84], however, they may make such radical sources more compatible.[246]

Pyrolysis

The ideas from flash pyrolysis, even if not directly applicable, can be transferred to conditions suitable for embedding radicals in helium droplets [67]. A scheme of the low-pressure, continuous, effusive pyrolysis source used at UNC is shown in Figure 2. The source can routinely be heated to 1800 K to produce clean effusive beams of radicals from appropriate precursor molecules. Due to the optical transparency of liquid helium over an extremely wide energy range (up to 21 eV), black-body radiation from the hot source does not effect the droplet beam.

Other schemes

While our approach has been to generate the radicals externally and dope them into the droplets, another approach would be to produce radicals from photolysis of a stable molecule already embedded inside a helium

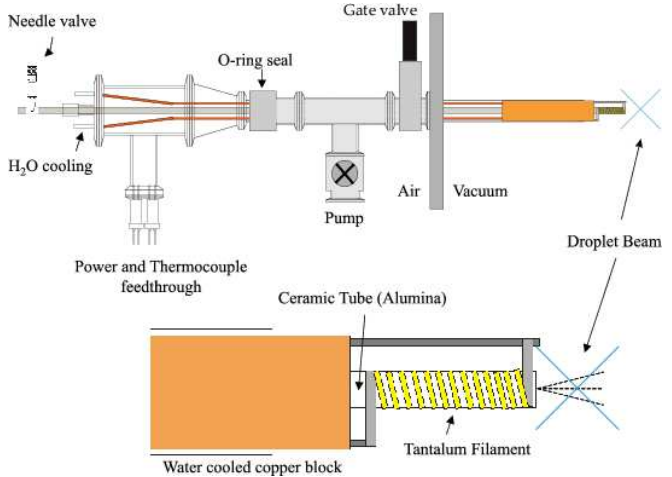


Figure 2: A schematic diagram of a pyrolysis source that can be load-locked into the helium nano-droplet apparatus, to facilitate the easy change of pick-up sources. In this case, an alumina tube is heated by a tantalum filament. A needle valve is used to regulate the flow of the precursor through the source.

droplet. Near threshold photo-dissociation of NO_2 has been attempted by Conjusteau *et al.* [85], with the goal of observing the $\text{NO}-\text{O}$ radical-radical van der Waals complex, but this has not been successful. It is unclear whether the helium is able to quench the energy faster than the time necessary to break the molecule apart, or the two fragments always react to give back NO_2 . Braun and Drabbels [86] have used 266 nm photodissociation of CF_3I and CH_3I embedded in helium droplets to study the translational dynamics of the recoiling CH_3 (CF_3) and I atom fragments. Here, 266 nm photolysis promotes the CH_3I to a highly repulsive electronic state, which is known to dissociate very rapidly in the gas-phase [87]. In the helium droplet study gas-phase fragments ejected from the droplets were detected by velocity map imaging [88] and their product distributions were found to be less anisotropic and shifted to lower velocities than compared to the equivalent gas-phase experiment [86], consistent with a model of hard sphere collisions. Since the detection method was based on imaging the gas-phase recoil products, studies were carried out using relatively small droplets, which allowed the fragments to escape. Photolyzing the embedding precursor in a much larger droplet, however, could allow one or both of the products to stay within the droplet.

Cold ion-molecule reactions have also been observed in helium droplets [89]. In this study 80 eV kinetic energy electrons were used to bombard the helium droplets, resulting in ionization of a single He atom in the droplet. The molecular impurity may then be ionized after resonant charge transfer [90]. Although the newly formed molecular ions are ejected from the droplet due to the energy released in the charge transfer step, ion-molecule reactions between these secondary molecular ions and ad-

ditional molecules embedded in the droplet could be observed, yielding, for example N_2D^+ (from N_2^+ and D_2), CH_4D^+ , or CH_3D_2^+ (from CH_4^+ or CH_3^+ and D_2) [89].

III. RADICAL MONOMERS IN HELIUM DROPLETS

A. Propargyl

The first spectroscopic study of a molecular radical in helium droplets was performed on propargyl (2-propynyl, C_3H_3) just five years ago [67]. In light of its role in sooting flames, the propargyl radical has been the focus of particular experimental attention [91–94]. Propargyl is one of the simplest conjugated systems with an odd number of electrons, also making it the focus of considerable theoretical study [95–98]. There is compelling evidence that propargyl is the most important radical precursor in the formation of benzene, polycyclic aromatic hydrocarbons, and soot in certain combustion processes [91–94, 99–104]. For example, the simple dimerization of two propargyl radicals is thought to be important in the formation of benzene, as suggested by Wu and Kern [99].

The work on the transient and very reactive propargyl radical embedded in helium droplets demonstrated how to couple our continuous, low-pressure pyrolysis source to a helium droplet beam for pick-up of such transient species [67]. From a fit to the rotationally resolved infrared spectrum of the ν_1 -transition the molecular parameters given in Table I are obtained. We find that the $K_a = 1$ states are populated due to nuclear spin statistics, confirming the C_{2v} symmetry of this radical. This shows, moreover, that the local environment inside the helium droplet does not lower the symmetry. Indeed, nuclear spin conversion processes are extremely slow in the gas-phase [108], but even the presence of the unpaired electron and the collision rich condensed phase environment inside the droplet does not induce any noticeable spin relaxation on the timescale of the experiment (~ 1 ms), demonstrating the weak perturbation of the embedded radical by the helium droplet environment. Nuclear spin relaxation was observed in quantum-solid para-hydrogen matrices on a much longer timescale of minutes to hours [109] and the accelerating effect of added ortho-hydrogen was clearly observed. Since the ensemble of complexes studied in a helium droplet experiment is only from droplets with exactly the wanted composition and the helium–complex interaction is generally weaker than the solid-hydrogen–molecule interaction, one would expect the conversion even to be considerably slower in helium droplets.

While the A rotational constants cannot be determined from the experimental data, the $(B + C)/2$ inertial parameters for ground and excited vibrational state were

constant	helium droplet ^a	gas-phase ^b
$A'' (\text{cm}^{-1})$	9.60847 ^c	9.60847 (18)
$(B'' + C'')/2 (\text{cm}^{-1})$	0.1198 (5)	0.312386 (12)
$B'' - C'' (\text{cm}^{-1})$	0.035 (2)	0.0105762 (35)
$\Delta''_N (\text{cm}^{-1})$	0.00042 (1)	$7.35 (122) \cdot 10^{-8}$
$A' (\text{cm}^{-1})$	9.60258 ^c	9.60258 (11)
$(B' + C')/2 (\text{cm}^{-1})$	0.1185 (5)	0.311641 (7)
$B' - C' (\text{cm}^{-1})$	0.035 (2)	0.010496 (13)
$\Delta'_N (\text{cm}^{-1})$	0.00062 (1)	$5.37 (76) \cdot 10^{-8}$
$\nu_0 (\text{cm}^{-1})$	3322.15 (1)	3322.292 (10)
$\mu''_a (\text{D})$	-0.150 (5)	—
$\Delta\mu_a (\text{D})$	0.02 (1)	—

^aReported helium droplet values are from reference 67. The values for $B - C$ were mistyped in the original publication and the corrected values are given here.

^bReported ground state values are from reference 105, excited state values are from reference 106.

^c A'' and A' are fixed at their respective gas-phase values.

Table I: Summary of the molecular constants for the propargyl radical in superfluid helium droplets [67], compared to those obtained in gas-phase studies [105–107]. Numbers in parenthesis are one standard deviation.

about one third of the gas-phase values, a reduction that is typical for rotational constants of this size [1]. The asymmetry-splittings $B - C$ are increased in the helium droplet environment, probably due to differential effects of the helium droplet environment on the rotation around the different axes.

This study was the first to experimentally determine the permanent dipole moment of propargyl radical by measuring the rotationally resolved infrared spectrum in the presence of a strong homogeneous electric field (50 kV cm^{-1}). It is known that dipole moments determined by Stark spectroscopy in helium droplets are very comparable to the gas-phase values [110]. This is confirmed by the good agreement of the measured values for propargyl ($\mu_0 = -0.150(5) \text{ D}$ and the $\Delta\mu_{v=1 \leftarrow 0} = 0.02(1) \text{ D}$) and calculated values ($\mu_e = -0.14(3) \text{ D}$, $\mu_0 = -0.124 \text{ D}$, $\mu_{v=1 \leftarrow 0} = 0.011 \text{ D}$) [96, 111].

B. Nitric oxide

Recently, the nitric oxide (NO) radical was studied using infrared diode laser spectroscopy in helium droplets [71]. Only the $Q(1/2)$ and $R(1/2)$ transitions of the $v = 1 \leftarrow 0$ transition in the $^2\Pi_{1/2}$ electronic ground state were observed due to the low temperature (0.4 K) of the droplet and the small moment of inertia of NO. From the line separation the rotational constant of NO in helium droplets is measured to be $B = 1.253 \text{ cm}^{-1}$, which is 76 % of the gas-phase value, in good agreement with previous closed shell systems of this size.

For the $Q(1/2)$ line sharp transitions are obtained. This reflects the fact that vibrational relaxation is slow due the absence of low-lying vibrational modes [112, and references therein]. Indeed, previous studies of HF embedded in helium droplets have shown that the monomer does not vibrationally relax at all on the timescale of the experiment (~ 1 ms) [113], so instead of depleting the droplet beam intensity, the extra vibrational energy of HF is simply carried to the bolometer. Using a mass-spectrometer based detection scheme, such as that used in the study of NO, one would not *a priori* expect a depletion signal in this case. Molecular absorption beam depletion can still be detected, however, due to pick-up of an impurity, i.e. a second NO or N₂, after the infrared excitation, leading to relaxation of the vibrationally excited molecular dimer, as shown conclusively for HF [112]. The resulting long monomer lifetime allows the nuclear hyperfine and Λ -doubling splittings of the transition to be resolved. The nuclear hyperfine splitting is unchanged from the isolated gas-phase value, whereas the Λ -doubling is increased by a factor of 1.55 compared to the gas-phase [71]. The authors discuss this effect in terms of electronic coupling and also suggest the possible influence of the helium density around the NO molecular axis [71]. For more details of these effects see the results on the NO-HF complex in section IV C and the general discussion of molecule-droplet interactions in section V.

The $R(1/2)$ line, on the other hand, shows a single unresolved band that fits well to a Lorentzian lineshape, which is attributed to fast rotational relaxation in the vibrationally excited state with a lifetime of $1.52 \cdot 10^{-10}$ s. The large rotational constant of NO places the excited rotational state in a region of high density of states for the fundamental excitations of the droplet, leading to a strong coupling and the corresponding short lifetime [1].

The NO molecule was also used as a sensitive probe of electronic effects of molecule-droplet interactions [114]. In that study, NO embedded in liquid helium droplets was photoionized and the ongoing dynamics was found to be quite complex. NO is initially excited by a two-photon excitation from its $^2\Pi$ electronic ground state to low-lying Rydberg states (NO^{*}). Subsequently, the nuclear degrees of freedom in NO^{*} and between the NO^{*} and the helium environment relax and NO^{*} is transported to the droplet surface on a time-scale shorter than the laser pulse (< 10 ns), where it can then leave the droplet along with a modest number of helium atoms or, alternatively, be photoionized. The formed ion can then be resolvated by snowball formation around the ion-core or leave the droplet surrounded by helium atoms.

C. Other species

Several other radicals or transient species have been observed in or on liquid helium droplets. For example

the spectra of individual open shell metal atoms on helium droplets have been obtained [4, 7, 115–117] and the chemiluminescence emission spectrum of the BaO^{*} product from the reaction $\text{Ba} + \text{N}_2\text{O} \rightarrow \text{BaO}^* + \text{N}_2$ inside a helium droplet has been observed [118]. The reaction was found to proceed very efficiently inside the droplet, and the influence of co-embedded xenon clusters was studied, which showed that the xenon pulls the nascent BaO, initially formed at the surface, into the center of the droplet. Experiments on the photodissociation of CF₃I to form CF₃ and I inside the helium droplets [86] and on ion-molecule reactions [89] were already discussed in section II B.

IV. RADICAL-CONTAINING MOLECULAR COMPLEXES

Whereas the effects of the moderately strong long-range electrostatic interactions in ion-molecule reactions are well known to have a significant influence on the associated reaction rates [119, 120], the importance of the weaker van der Waals forces in the entrance channels of neutral reactions have been only recently fully appreciated [38, 41, 121, 122]. Experimental and theoretical work on the $\text{Cl} + \text{HD} \rightarrow \text{HCl}(\text{DCl}) + \text{D}(\text{H})$ reaction shows that the torque experienced by the HD in the entrance valley of the potential has a significant effect on the overall reaction rates and branching ratios [31–34]. Furthermore, the rotational excitation of HCl products formed from abstraction reactions of chlorine and organic molecules, for example, can only be accurately described by taking into account the features of the exit channel. The dipole-dipole interaction of the departing fragments was found to be very important in determining the product final state distributions [38]. For the dissociation of formaldehyde a completely new dissociation mechanism (*roaming hydrogen atom* mechanism) has been proposed [36, 37]. These results are clear examples, that entrance and exit channel complexes of molecular reactions probe the associated PES at energies that are relevant to the systems' chemical reaction dynamics, despite being much lower in energy than the corresponding transition states. However, the torque on the reactants at long range acts to deflect trajectories towards or away from the transition state [33]. Therefore, these complexes are of considerable importance in understanding the nature of the reactions, particularly at low translational energies (low temperatures).

The isolation and stabilization of entrance and exit channel complexes in liquid helium droplets and their high-resolution spectroscopic study provides a novel experimental approach for studying these important systems. In the remainder of this section we will summarize the experiments performed on such complexes in liquid helium droplets to date. In the first part we will discuss the hydrogen-bound complexes of halogen atoms with small

linear molecules and in the second part of this section we will proceed to complexes of hydrocarbon radicals with hydrogen acids.

A. Complexes containing halogen atoms

Recently, a large series of complexes of closed shell molecules with halogen atoms embedded in liquid helium droplets have been studied using high-resolution infrared spectroscopy, i. e. the complexes of chlorine, bromine, and iodine with HF and HCN, respectively [123, 124]. These systems represent the prototypical *heavy—light-heavy* X-HY (X=Cl, Br, I; Y=F, CN) complexes which serve as prominent benchmark systems for the understanding of elementary reaction dynamic studies. They can be studied in great detail theoretically [125–138], as they contain only two heavy atoms (X-HF) and only a few nuclear degrees of freedom. Some stationary points of such systems have also been studied experimentally, for example, by spectroscopy of the transition states [134, 139–141] and using infrared spectroscopy in noble-gas matrices [142–144]. These studies, however, did not reveal detailed information on the associated entrance or exit channel regions of the reactions.

The X-HF [145–150] and X-HCN [151–153] PES have also been studied in collision experiments. Recently, strong rotational enhancement has been described for the F + HCl reaction [150, 154]. The chemiluminescence from HF produced in chemical lasers, i. e. from reactions of ClF with hydrogen, has been observed [155]. However, so far no spectra of the stationary points on the PES have been obtained for the free molecular complexes.

For these X-HY systems, the interaction of the quadrupole moment of the halogen atom with the dipole moment of the molecule suggests two linear structures with the atom sitting on either end of the linear molecule. However, T-shaped minima are also predicted due to the considerable quadrupole moments of the molecules [125, 130, 131, 133, 138]. The weak interaction between a halogen atom and the molecules in a van der Waals complex suggests, that, to a first approximation, the orbital angular momentum j_A of the atom will be conserved in the complex. This interaction removes the degeneracy of the 2P atomic states, which in C_s symmetry gives rise to two states of A' and one state of A'' symmetry. These correspond to the three relative orientations of the singly occupied orbital with respect to the complexation partner, i. e. the unpaired electron being in the p_x , p_y , and p_z orbital, respectively. Solving for the eigenvalues of the electronic Schrödinger equation under the Born-Oppenheimer approximation yields the adiabatic PES. However, since these surfaces are coupled by non-adiabatic coupling terms originating from the nuclear kinetic energy operator, it is often helpful to solve for the bound states in a diabatic representation

[133, 138]. The electronic anisotropy is further complicated due to electron spin, and spin-orbit coupling can also have an important effect on shaping the PES. For comparison we reproduce the lowest diabatic and adiabatic PES including spin-orbit coupling for the Cl-HCl, Cl-HF, and Br-HCN complexes in Figure 3(A–C), (D–F), and (G), respectively. The results for Cl-HCl [132, 133] and Cl-HF [136, 137] have been published previously, while preliminary results for Br-HCN have been provided by A. van der Avoird. The general topology of the Cl-HCl and Cl-HF surfaces are quite similar. However, the larger dipole of HF, compared to HCl, makes the linear hydrogen bound minimum deeper for Cl-HF and the T-shaped minimum has almost completely disappeared in the lowest adiabatic surface. Indeed, for Cl-HF only the linear hydrogen bound isomer was observed experimentally in helium droplets, suggesting that the T-shaped or linear HF-X isomers are not formed. Detailed comparisons of the experimental and theoretical results for the X-HF systems have been given elsewhere [124, 131, 136, 137]. In contrast, the lowest adiabatic surface for the Br-HCN system shows two deep minima corresponding to the hydrogen-bound and nitrogen-bound linear isomers, respectively, which are also both observed experimentally [123].

The $1^2A'$ and $1^2A''$ surfaces are degenerate at the linear H-bound configuration ($\theta = 0$), whereas the $1^2A'$ and $2^2A'$ surfaces are degenerate at the linear N-bound configuration ($\theta = 180$). Therefore, the electronic symmetry is $^2\Sigma$ for HCN-X, with the unpaired electron along the axis of the molecule, and $^2\Pi$ for X-HCN, with the unpaired electron perpendicular to the axis of the molecule.

In Figure 4 survey scans for the Br-HCN systems with cold (room temperature) and heated (~ 1600 K) pyrolysis source are shown as an example. Such overview scans are infrared depletion spectra obtained in the presence of strong homogeneous electric fields (~ 60 kV cm $^{-1}$) in which the complete rotational structure is collapsed into a single *pendular* transition [68, 156, 157] due to the large degree of orientation of the polar molecules in the cold environment.

When the pyrolysis source is cold, only complexes of HCN with halogen molecules are formed. When the pyrolysis nozzle is heated, however, the signals associated with the precursor complexes are significantly reduced, due to the dissociation into atoms, and a new set of signals is observed to grow in, which are readily assigned to binary complexes of bromine atoms with HCN. Based on harmonic vibrational frequency calculations as well as physical intuition, the largely different frequency shifts of the ν_{CH} stretching vibrations result from the two different structures of the complexes, namely the peak shifted furthest to the red corresponds to the Br-HCN complex, and the peak which exhibits only a small shift is related to the HCN-Br complex. This assignment is confirmed by analysis of the field-free spectra of each of these transitions [123, 158].

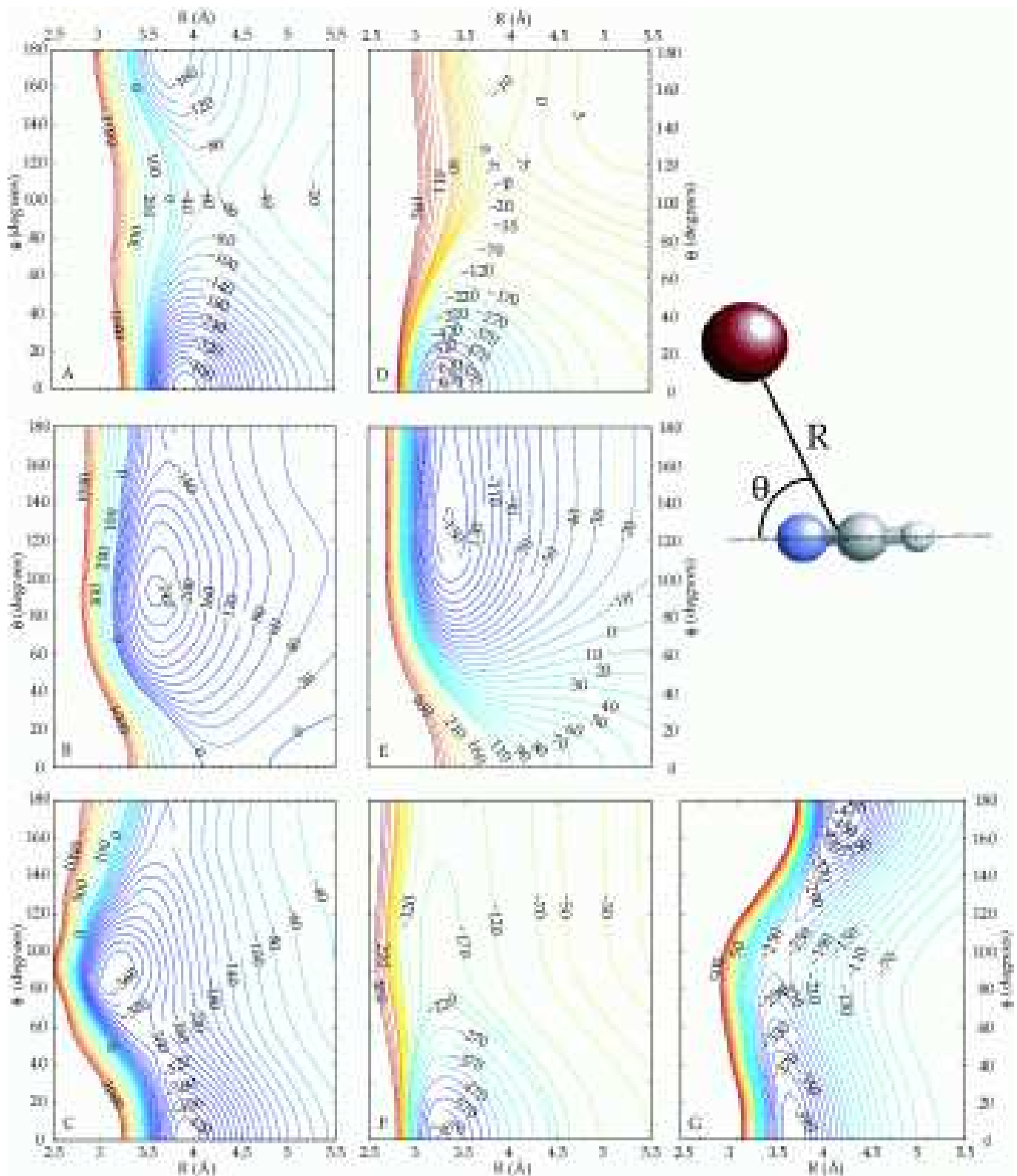


Figure 3: (A, D) Diabatic potential energy surfaces for Cl-HCl and Cl-HF $j_A = 3/2$ $\omega = 3/2$ and (B, E) $j_A = 3/2$ $\omega = 1/2$, respectively. (C–F) The lowest adiabatic potential energy surface including spin-orbit coupling for Cl-HCl (C), Cl-HF (F), and Br-HCN (G), respectively. Jacobi coordinates as shown in the inset have been used throughout and $\theta = 0^\circ$ corresponds to the hydrogen bound arrangement. See text for details.

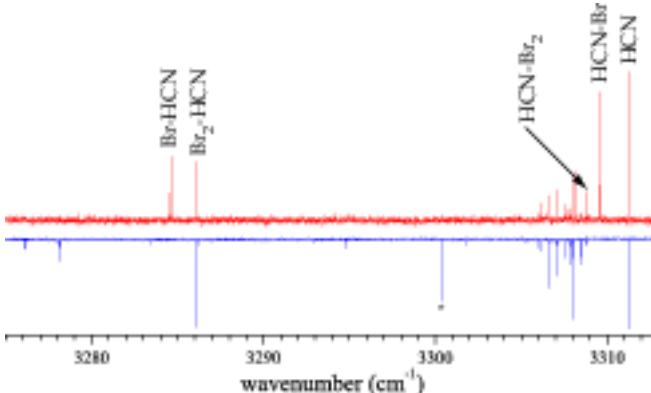


Figure 4: Pendular survey scans revealing the pyrolysis source temperature dependence (upward peaks are with a hot source, downward peaks are with a cold source) for the HCN + bromine experiment. The scans show peaks which we identify as molecular and atomic bromine complexed with HCN. The peak labeled with an asterisk is a known impurity.

In Figure 5 the field free spectrum of Br-HF is shown as an example. The vibrational frequency is shifted by 131 cm^{-1} to lower energy compared to the HF monomer transition [113], indicating the binding of Br to the hydrogen end of HF. The simulation of the rotationally resolved spectrum, constituted by all the individual simulated transitions shown at the bottom of the figure, reproduces all of the important features of the spectrum. Some deviations are observed especially for the lowest- J transitions, an effect that is regularly observed for molecules embedded inside helium droplets; see section V for details. The overall structure and all features are clearly reproduced by the simulation. Therefore, these spectra confirm the $^2\Pi_{3/2}$ ground states of these hydrogen bound complexes, consistent with the $^2P_{3/2}$ ground state of atomic bromine. Spectra and simulations of the same quality are obtained for all other hydrogen bound X-HF/HCN complexes studied. The molecular parameters obtained for the ground states for all complexes are given in Table II. In Figure 6 the field-free spectrum of the nitrogen-bound HCN-Br complex is shown for a comparison and the molecular constants of all corresponding HCN-X complexes are also given in Table II. These nitrogen-bound complexes exhibit quite different features than the hydrogen bound complexes. Whereas the ν_{CH} vibrational frequencies are shifted by tens of wavenumbers for the hydrogen bound complexes, these N-bound complexes are shifted only by a few cm^{-1} compared to the free HCN molecule. The rotationally resolved spectra of the HCN-Br and HCN-I complexes also show a very different fine-structure, which is assigned to parity-splitting due to the spin-orbit interaction between the $^2\Sigma_{1/2}$ and the $^2\Pi_{1/2}$ states of the complex [123, 158]. For the HCN-Cl complex no such fine-structure could be observed, what is consistent with the much smaller spin-orbit coupling constant of atomic chlorine than for bromine and iodine and the correspondingly small split-

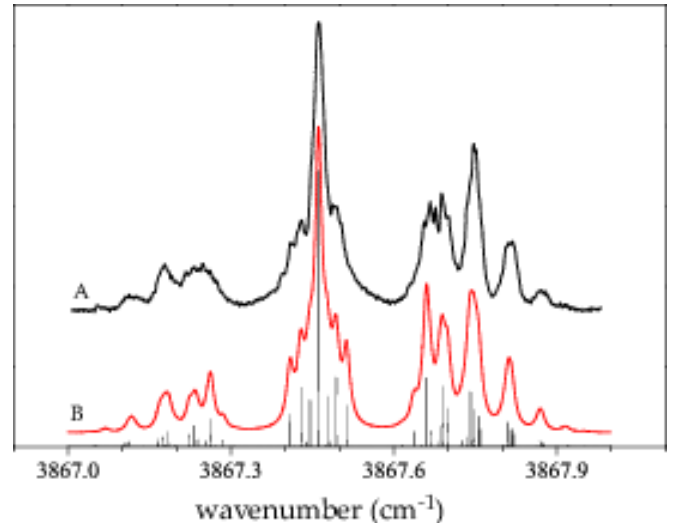


Figure 5: (A) The field-free infrared spectrum of Br-HF shown together with (B) a simulation that includes nuclear magnetic hyperfine interactions due to the bromine nucleus ($I = 3/2$). The stick spectrum shows all of the transitions that underlie the observed features.

tings of the transitions that are not visible at the resolution of our experiment.

It had been proposed that Cl-HCl complexes may possess T-shaped structures, but display several of the properties of a linear open-shell molecule [133]. Given the frequency shift from the HF monomer, however, this is un-

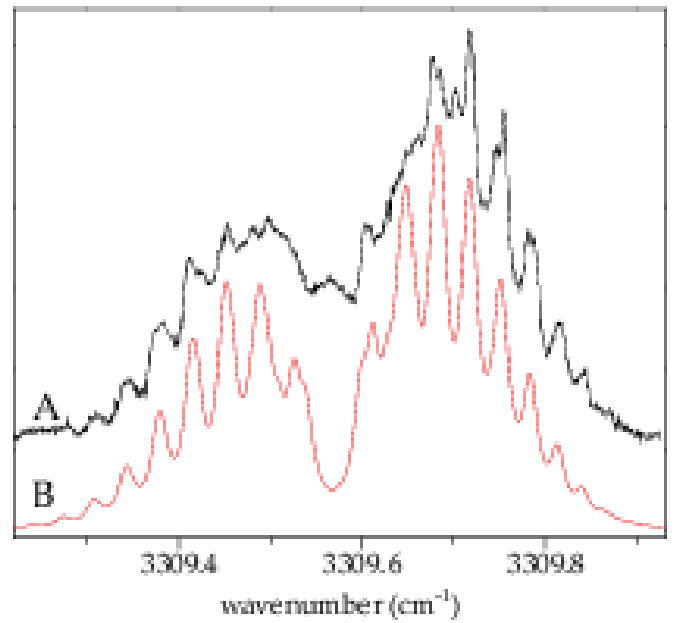


Figure 6: (A) The field-free infrared spectrum of HCN-Br shown together with (B) a simulation that includes parity splitting induced by spin-orbit coupling of the $^2\Sigma_{1/2}$ and the $^2\Pi_{1/2}$ states of the complex.

species	ν_0 (cm $^{-1}$)	B ^a (cm $^{-1}$)	D (10 $^{-4}$ cm $^{-1}$)	μ (D)	$a\Lambda + (b+c)\Sigma$ (cm $^{-1}$)	isotope splitting ^b (cm $^{-1}$)	$B_{\text{gas}}/B_{\text{He}}$ ^c
$^{35}\text{Cl-HF}$	3887.54	0.055	1.2	1.9	0.005	0.038	2.3
$^{79}\text{Br-HF}$	3867.46	0.043	0.95	2.1	0.045	0.010	2.2
I-HF	3847.82	0.037	0.3	2.2	0.035	—	2.2
Br-HCN	3284.61	0.0151	1.5		0.04	^d	2.7
I-HCN	3277.79	0.0120	1.0		0.04	—	2.83
HCN-Cl	3309.33	0.032	0.50	3.0	—	0.001 ^d	2.7
HCN-Br	3309.55	0.019	0.12	3.78	—	^d	2.75
HCN-I	3309.37	0.016	0.10	(3.91) ^e	—	—	2.75

^aFrom references 123, 124

^bThe frequency of the heavier complex subtracted from the corresponding one of the lighter isotopologue.

^cGas-phase values are from *ab initio* calculations [123, 124]. For the HCN-X complexes the gas-phase values are B_0 values from one-dimensionally spin-orbit corrected adiabatic PES [123].

^dNo isotope splitting is observed experimentally, which is consistent with bound state calculations on an one-dimensional *ab initio* potential energy surface for HCN-Cl; splittings for the bromine complexes are expected to be even smaller [123].

^e*ab initio* value from reference 123

Table II: Ground states molecular parameters from infrared spectroscopy for all complexes of HF and HCN with halogen atoms observed so far [123, 124]. For chlorine and bromine the constants of the lighter isotopologue are given (iodine has only a single isotope) and the isotope splittings are the frequency of the lighter isotopologue subtracted from the frequency of the heavier one.

likely the case for the X-HF complexes observed here; see reference 124 for a detailed discussion. Nevertheless, the fact that this point is subject of considerable debate illustrates how poorly we still understand these species, calling out for more experiments and theory on these entrance channel complexes.

No complexes of atomic fluorine with HF or HCN have been observed, despite extensive searches for such complexes and a previous assignment for the ν_{HF} stretching vibrations of F-HF in argon matrices [144]. Moreover, from *ab initio* calculations it is clear, that the reaction of F + HCN to form HFCN via an insertion mechanism is quite exothermic and exhibits only a small barrier, if at all [123, 158]. The fact that the fluorine containing F-HCN complexes cannot be observed, could indeed be an indication that the insertion reaction takes place, even at 0.37 K. This reasoning is also supported by argon matrix work where the insertion product has been observed, whereas no pre-reactive (van der Waals) complexes were found [159, 160]. Guided by the experimental vibrational frequency of 3018 cm $^{-1}$ for HFCN in solid argon, we also searched for the HFCN reaction product in the helium droplets. However, since this frequency is at the edge of the F-center laser tuning range and the transition strength is about 50 times weaker than for the HCN monomer, no manifestations of the HFCN product could be observed. Revisiting the experiment using newer technology OPO lasers [158, 161, 162], which have enhanced tuning ranges and improved power, might show the corresponding spectral signatures.

Similar studies to the ones described here have also been performed on the pre-reactive complexes of open-shell metal atoms (Al, Ga, In) [158] and semiconductor atoms (Ge) with HCN and preliminary results were presented in an earlier review [1]. Upon complex formation in liquid helium droplets the same linear van der Waals com-

plexes as for the halogen atom HCN complexes are observed. However, these atom-HCN complexes can undergo an exothermic insertion reaction and the corresponding barriers are low enough that the reactions do actually proceed even at the low ambient temperatures of the helium droplet, depending on the metal, either directly or initiated by a single-quantum excitation of the ν_{CH} stretching vibration in the HCN moiety. Details on the van der Waals complexes and the insertion products will be published elsewhere [163]. Furthermore, the complexes of HCN with several alkaline (Na, K, Rb, Cs) and earth alkaline (Mg, Ca, Sr) atoms [164, 165], with Zn atoms [166], and with Cu and Au atoms have been observed. The complexes of one to six magnesium atoms with several small molecules have been studied extensively [167–170]. Due to the electronic quasi-closed shell structure of magnesium and high barriers to reaction in these systems, these complexes exhibit the simple spectra of closed shell van der Waals complexes. For the heavier atoms from these series it is known that the atom resides on the surface of the droplet, forming a dimple [2, and references therein]. It is interesting to study the effects of embedding an atom that wants to stay on the surface of the droplet, and a molecule that wants to be inside the droplet, which, in addition, strongly attract each other. For Na-HCN, one of these systems, a very strong absorption line is observed [164, 165]. The remaining rotational structure, however, is the spectrum of a linear or spherical top with a very much larger inertial moment than that expected for a Na-HCN binary complex, even inside a helium droplet. The spectrum is actually consistent with the rotation of the Na-HCN mass around the droplet and the observed rotational constant scales nicely with the droplet radius. Therefore, it is concluded, that the sodium pulls the HCN into a dimple on the surface of the droplet and the complex can freely rotate over the surface of the helium droplet [164, 165]. However, no

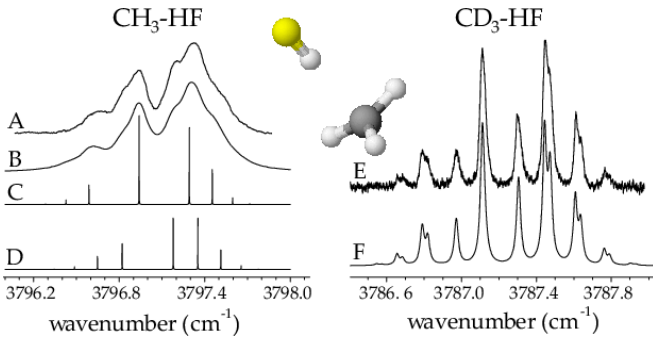


Figure 7: (A) An experimental spectrum corresponding to the HF stretching vibration of the $\text{CH}_3\text{-HF}$ molecular complex, along with a symmetric top simulation (B) which clearly shows the C_{3v} symmetry of this complex. In (C) and (D) we plot the contributions from the $K=1$ and $K=0$ bands respectively, illustrating that the nuclear spin statistics prevent interconversion of these two manifolds of states. Scan (E) shows the corresponding spectrum for CD_3 radicals, illustrating a dramatic increase in the lifetime of the complex and (F) the corresponding simulation.

rotational fine-structure can be observed due to the unresolved features in the extremely small B spectra. The spectra of the heavier atoms (K, Rb, Cs, Ca, Sr) show similar effects; for some of them even both species can be observed simultaneously – an embedded van der Waals complex as for Mg-HCN and a surface-bound complex as for Na-HCN [164, 165].

B. Complexes of hydrocarbon radicals

1. Complexes of methyl radical with HF and HCN

The reactions of hydrocarbons are of particular interest due to the wide range of reactions for which they play a key role, for example combustion processes [8]. The hydrogen exchange reaction with fluorine atoms form a basis of our understanding of much larger systems. The most simple fluorine + hydrocarbon system, $\text{F} + \text{CH}_4 \rightarrow \text{HF} + \text{CH}_3$, has been extensively studied both experimentally [171] and theoretically [172], however, high-resolution spectroscopic studies of the entrance and exit channel regions of the PES are still lacking. Previous studies have identified the $\text{CH}_3\text{-HF}$ complex in argon matrices [52, 173–175].

In order to probe the exit channel region of the PES, methyl radicals have been produced via pyrolysis, while a second pick-up cell was used to dope the droplet with an HF molecule. Azomethane, di-tert-butyl peroxide (DTBP), and CH_3I were all used as precursors to confirm that the signals genuinely arose from CH_3 . In addition, several transitions of the CH_3 monomer were also observed in helium. Figure 7 (A) shows a partially rotation-

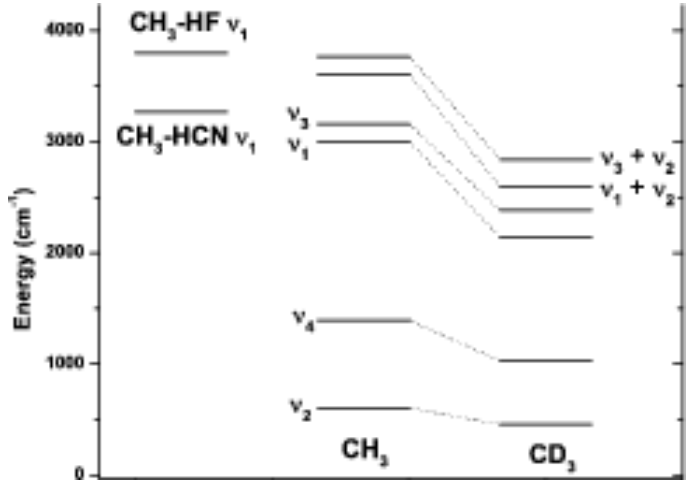


Figure 8: A plot of the corresponding energy levels of the CH_3 and CD_3 monomers. The effect of deuteration in the $\text{CD}_3\text{-HF}$ complex is to lower the vibrational frequencies of the CH stretches, effectively quenching the vibration-vibration resonance that occurs with the excited HF stretching state of the complex. See text for details.

ally resolved experimental spectrum which is assigned to the HF stretching vibration of the $\text{CH}_3\text{-HF}$ molecular complex. The C_{3v} symmetry of the complex can be uniquely identified from the large Q branch present in the spectrum. Indeed, at the temperature of the droplets, we would not normally expect population of the excited K states since the rotation about the a -axis only moves the three hydrogen atoms, giving rise to a large energy spacing between different K states. Assuming nuclear spin conversion is slow compared with the timescale of the experiment, the nuclear spin statistics of the ro-vibrational wavefunction treat the $K = 0, 3, 6 \dots$ and $K = 1, 2, 4, 5, 7 \dots$ states as separate identities of A and E symmetry, respectively, and thus they do not interconvert upon cooling to 0.37 K. At the temperature of the droplets, all of the population is cooled into the $K = 0$ and $K = 1$ states, and only for the $K = 1$ states $\Delta J = 0$ transitions are allowed. The intensities reflect the population of $A : E$ states of CH_3 in the high-temperature source, yielding a $\sim 1 : 1$ population ratio for the $K=0$ and $K=1$ bands.

The linewidths in the $\text{CH}_3\text{-HF}$ spectrum are rather broad, somewhat limiting the accuracy of the molecular parameters determined by the fit to the spectrum, shown in Figure 7 (B)–(D). Considering the cause of the broadening we concluded that a vibration-vibration resonance was the likely cause of the shortening of the excited state lifetime, coupling the HF stretch excited state to the CH_3 stretches of the methyl radical. To test this idea, we also recorded the spectrum of $\text{CD}_3\text{-HF}$, which is shown in Figure 7 (E). CD_3 radicals were produced by pyrolysis of CD_3I . Deuteration of CH_3 lowers the frequencies of the vibrations as shown in Figure 8, detuning the resonance, and resulting in much narrower lines, as expected. The

molecular parameters derived from the fits to the spectra are summarized in Table III.

In addition to the importance of the long-range van der Waals forces in giving the reactants a torque, which may be towards or away from the transition state [31–35], the stabilization of weakly bound reactive complexes may represent an ideal starting point for the study of reactive resonances [17]. The experimental observation of reactive, or Feshbach, resonances in chemical reactions are highly sought after because they result from purely quantum mechanical effects and probe regions of the PES which are typically not sampled by current experimental techniques. Such resonances result from a coupling of the vibrationally adiabatic PES near the transition state, giving rise to dynamical trapping. To date, reactive resonances have been confirmed in the crossed molecular beam reactive scattering of $F + H_2 \rightarrow HF + H$ [17] and the photo-electron spectrum of IHI^- [176]. Resonances of this type are not expected to be constrained to such simple systems, it is only our ability to detect or recognize them, which has limited current experiments to such simple systems. Only recently has a reactive resonance been implicated in a true polyatomic reaction, namely $F + CH_4 \rightarrow HF + CH_3$ [171]. At low collision energies the transient resonance in this reaction can proceed via predissociation into $HF(v = 2, j') + CH_3(v = 0)$, similar to $F + HD$ [17]. The extra degrees of freedom of the CH_3 , however, may allow intramolecular vibrational energy relaxation (IVR) which would shorten the resonance lifetime, allowing the $HF(v = 2) + CH_3(v_1 = 1)$ channel to compete effectively with the pre-dissociative decay described above. At higher collision energies the decay of the resonance state into $HF(v = 3) + CH_3(v = 0)$ dominates [171].

From our experiments on the CH_3 -HF and CD_3 -HF complexes we can confirm a similar coupling between the $HF(v = 1) + CH_3(v_1 = 0)$ and $HF(v = 0) + CH_3(v_1 = 1)$ states, as indicated by the vibration-vibration resonance lifetime, which is considerably shortened in the case of CD_3 -HF. Overtone pumping of the CH_3 -HF van der Waals complex may allow access to the region of the PES directly involved in the reactive resonance, as proposed for $F + H_2$ [17].

In order to further experimentally explore the V-V coupling mechanism observed for the CH_3 -HF complex, one can also alter the energy of the bright state by changing the identity of the chromophore. Rotationally resolved infrared spectra have been recorded for the CH_3 -HCN and CD_3 -HCN complexes [177]. As seen from the energy level diagram in Figure 8, the CH stretching frequency of HCN lies below the combination levels of the CH_3 monomer, implicated in the relaxation of CH_3 -HF, so a more direct comparison of the coupling can be made with just the ν_1 and ν_3 levels of CH_3 . Interestingly for CD_3 -HCN, the combination band for CD_3 is a viable relaxation channel. The peaks in the CH_3 -HCN spectrum are well fit by a Lorentzian lineshape, just

as in CH_3 -HF, suggesting that the broadening results from the finite lifetime of the excited state. Comparing the observed linewidths for CH_3 -HCN and CH_3 -HF we find that the lifetime of CH_3 -HCN is approximately two times longer than for CH_3 -HF, suggesting that the coupling to the combination band is indeed the important relaxation channel for CH_3 -HF. The CD_3 -HCN molecular complex exhibited linewidths which were only slightly smaller than for CH_3 -HCN, clearly showing that the effect of coupling to the CH stretches of the CH_3 directly is much smaller.

To our knowledge no studies have investigated the possibility that combination modes are excited in the $F + CH_4$ reaction, other than pure overtones. Based on our observed coupling of the $HF(v = 1) + CH_3(v = 0)$ to $HF(v = 0) + CH_3(v_1 = 1 \text{ or } v_3 = 1 + v_2 = 1)$ it may be possible to observe this reaction channel in an crossed molecular beam reactive scattering experiment similar to the ones reported by the group of Kopin Liu [171, 178], where the experimental conditions favor the production of methyl in the CH-stretch excited state, i. e. near threshold.

2. Larger hydrocarbon radicals

Larger hydrocarbon radicals, including ethyl (C_2H_5) and allyl (C_3H_5) radicals, may be readily formed by pyrolysis of their corresponding iodine precursors [74, 179–181], and spectra have been recorded for their complexes with HCN and HF embedded in helium droplets. These systems are of interest since they may be directly compared with the methyl radical complexes observed previously. Figure 9 shows a pendular survey scan for the HF stretching region. In the bottom trace C_2H_5I is flowed through a room temperature pyrolysis source, and the peak at 3747 cm^{-1} is assigned to a C_2H_5I -HF complex. Upon heating the source, this peak is observed to decrease in intensity, and a new strong peak is observed at 3774 cm^{-1} which we assign to a C_2H_5 -HF complex. Turning off the electric field we recover the rotationally resolved spectrum shown in Figure 10 (A). Figure 10 C) shows the Stark spectrum for this band recorded at an electric field strength of 3.86 kV cm^{-1} . The molecular parameters determined from the fits to the spectra are given in Table III, together with the values for the ethyl-HCN complex. In Figure 11 (A) and (C) the field free spectrum and the Stark spectrum of the allyl radical-HF complex are shown, respectively. Still for a molecule of that size clear rotational structure is observed and the obtained molecular parameters are summarized in Table III, together with the values for the allyl-HCN complex. The results on these larger hydrocarbon radicals are very promising for studying radicals that are even more important in radical chain reactions in combustion processes, such as, for example, $C_nH_{2n+1}OO$ peroxy-radicals, which are some of the most important intermediates in these reactions [182]. High resolution

species	ν_0 (cm $^{-1}$)	A (cm $^{-1}$)	ΔA (cm $^{-1}$)	$(B + C)/2$ (cm $^{-1}$)	D_J (cm $^{-1}$)	μ (D)
CH ₃ -HF	3797.00		0.06 ^a	0.09	$2.5 \cdot 10^{-4}$	2.6
CD ₃ -HF	3787.14		0.027 ^a	0.083	$2.6 \cdot 10^{-4}$	2.6
C ₂ H ₅ -HF	3774.45	0.30		0.059	$4.8 \cdot 10^{-5}$	2.7
C ₃ H ₅ -HF	3810.10	0.095		0.040	$1.0 \cdot 10^{-4}$	2.4
CH ₃ -HCN	3265.70		0.04 ^a	0.030	$3.7 \cdot 10^{-5}$	3.1
CD ₃ -HCN	3262.09		0.018 ^a	0.027	$2.6 \cdot 10^{-5}$	3.1
C ₂ H ₅ -HCN	3260.29	0.30		0.15	$2.9 \cdot 10^{-5}$	4.1
C ₃ H ₅ -HCN	3260.14	0.09		0.016	$8.0 \cdot 10^{-6}$	3.2

^aThese parameters are taken from gas-phase work [52, 173].

Table III: Ground-state experimental molecular constants of hydrocarbon-HF and -HCN complexes. Comparison to *ab initio* inertial parameters shows reduction factors for the rotational constants like closed shell systems of the same size [1].

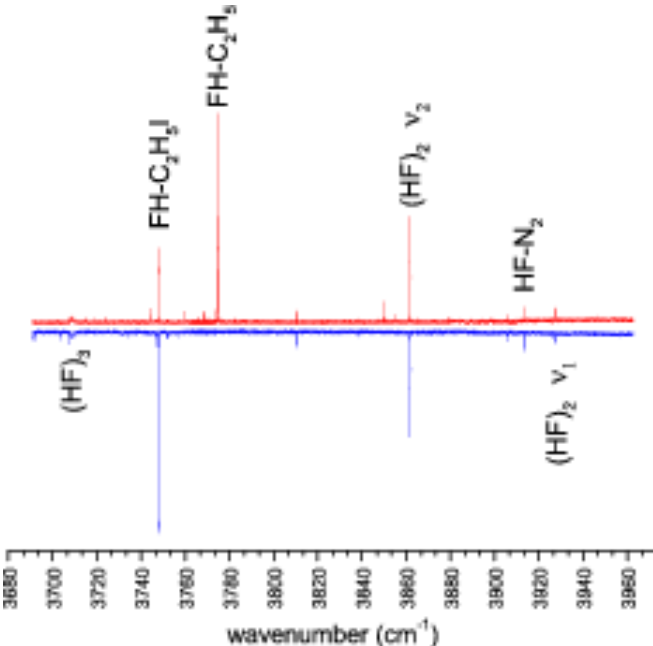


Figure 9: Pendular survey scans corresponding to flowing ethyl iodide through a cold (downward going peaks) or hot (upward going peaks) pyrolysis source. HF is then picked up downstream in a separate pick-up cell. We assign the peak at 3747 cm $^{-1}$ to an HF-C₂H₅I complex, the intensity of which decreases substantially at temperatures appropriate for pyrolysis. At pyrolysis temperatures of about 1000 K, the peak at 3774 cm $^{-1}$ appears which is assigned to the HF-Ethyl radical complex.

spectra of these molecules have been difficult to obtain in free-jet expansions, though [183–188].

Moreover, given that we have shown that pure effusive beams of hydrocarbon radicals can be made under suitable conditions for helium droplet pick-up, the possibility of studying radical-radical and radical-molecule reactions inside the helium droplets is reasonable. A very interesting and simple experiment would be to dope a single oxygen molecule into a droplet containing a hydrocarbon

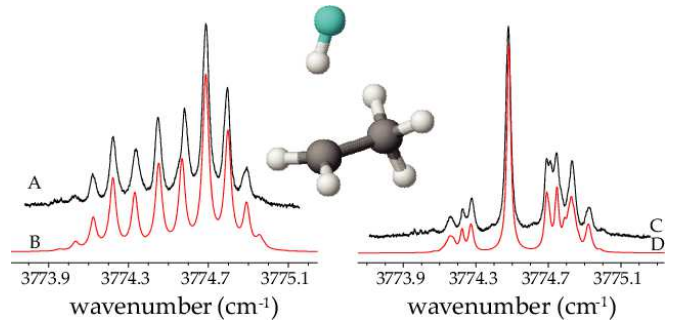


Figure 10: Rotationally resolved field-free (A) and Stark (C) spectra corresponding to the HF stretching vibration of the HF-C₂H₅ complex and the corresponding simulations, (B) and (D), respectively.

radical. Theoretical calculations predict that the reaction to form hydroperoxy radicals (ROO $^{\bullet}$) is barrierless [189], however, at low temperatures this might only apply if the oxygen directly approaches the radical center. Instead, the helium might trap the complex in a local van der Waals minimum, forming a pre-reactive complex, similar to what is discussed in section VIA. Vibrational excitation could then be used to initiate the corresponding reaction.

C. NO-HF

Given the recent observation that the Λ doubling of NO was increased by 55 % upon solvation in a helium droplet, there is considerable need to further study this phenomenon, since exciting new molecules and clusters might only be formed in helium, with no gas-phase data available for comparison. This statement is already particularly true given our preliminary results on open shell clusters with Br, I, Ga, and In atoms which have revealed large parity splittings. Indeed, recent high-level theoretical calculations on the HCN-Br complex indicate that the parity splitting is much smaller in a helium droplet than

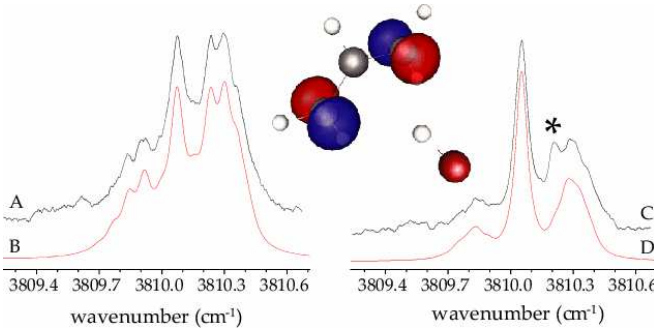


Figure 11: Field-free (A) and Stark (C) spectra for the HF-Allyl radical complex, and the corresponding simulations, (B) and (D), respectively. The peak marked with an asterisk corresponds to a known impurity which overlaps at this frequency.

one might expect in the gas-phase [190]. The electronic angular momentum couplings, which are responsible for such open-shell effects, are very sensitive probes of excited electronic states. Moreover, there is relatively little

information available so far on how the helium droplet effects these.

To further our understanding of such open shell species in helium, we have recorded the infrared spectrum of the NO-HF complex, which has been observed previously in the gas-phase by Fawzy *et al.* [191]. While NO-HF is a bent complex, we can use a diatomic, or more generally, a linear molecule Hamiltonian to describe the $|\Omega| = 1/2$ levels just as one can use a closed shell linear rotor Hamiltonian for the $K = 0$ levels of a symmetric top. If we take P as the projection of the total angular momentum on the a -axis of the complex, then we are considering only the $|P| = 1/2$ levels. Since NO-HF is only slightly bent away from linearity, these excited P states are of significantly higher energy and are not populated at the rotational temperatures typical of molecular beams or helium droplets. The observed spectrum in the gas phase is dominated by pairs of transitions, reminiscent of Λ -type doubling. In their original model, the rotational energies were obtained by fitting the spectrum using

$$F(J) = BJ(J+1) - DJ^2(J+1)^2 \pm \frac{1}{2}[p(J+\frac{1}{2}) - p_J(J+\frac{1}{2})J(J+1)] \quad (1)$$

where J is half-integer, starting at $J = 1/2$, and the $-$ and $+$ signs in front of the square bracketed term are defined for the e and f parity sub-states, respectively. B and p are the rotational and parity doubling constants, respectively, and D and p_J are the corresponding centrifugal distortion parameters. Fitting the helium droplet spectrum to the same model Hamiltonian resulted in the molecular constants listed in Table IV, which are compared with the gas-phase values [191]. In contrast to NO in helium, we find that for NO-HF, the parity constant p , is reduced from the gas-phase value by exactly the same amount (within experimental uncertainty) as the rotational constant B . As pointed out for NO [71], the expression for the parity splitting does have a linear relationship with B , and this is exactly what we see for NO-HF. For NO monomer, however, the parity splitting was increased by 55 % despite the fact that the rotational constant was 76 % of the gas-phase value, illustrating that the mechanism with which the helium interacts with the molecule is different [71].

	constant (cm^{-1})	helium droplet	gas-phase
ν_0	3871.76	3877.47269(12)	
B''	0.0473	0.111320(17)	
B'	0.0479	0.116167(19)	
p''	0.0676	0.15274(19)	
p'	0.0802	0.19652(18)	
D''_J	1.25×10^{-4}	$2.56(31) \times 10^{-6}$	
D'_J	1.43×10^{-4}	$2.56(31) \times 10^{-6}$	
p''_J	3.8×10^{-4}	$0.932(54) \times 10^{-4}$	
p'_J	4.2×10^{-4}	$0.503(38) \times 10^{-4}$	

Table IV: Molecular constants of the NO-HF complex derived by fitting the experimentally observed spectrum for the HF stretching vibration in both helium droplets and in the gas-phase [191]. The fit to the field free spectrum was performed using the contour fitting routines in pgopher [192]. Note that in pgopher the signs of p_J must be reversed when compared to the origin model of Fawzy [191].

V. INTERACTIONS BETWEEN HELIUM DROPLETS AND EMBEDDED MOLECULES

Since the first spectroscopic investigation of SF_6 embedded in helium droplets in 1992 [193] and the first observation of free rotation thereof a few years later [59], a

large number of molecules and cluster systems have been studied and trends are now being established. The most easily recognized and well publicized trend is the effect of the helium droplet on the associated rotational constants of the embedded cluster. Two dynamical regimes have been established. Light rotors with their large rotational constants do not couple efficiently to the helium, resulting in only a slight decrease in the observed rotational constant compared to the gas phase. In contrast, heavier rotors typically exhibit a much more anisotropic interaction with the helium, which allows some of the helium to follow the rotational motion, thus adding to its moment of inertia. Typically rotational constants of *heavy* rotors ($B < 1 \text{ cm}^{-1}$) are reduced by a factor of 2.5 ± 0.5 when compared to the gas-phase [1]. The scatter in the reduction factors of the rotational constants results from the unique dopant-helium interactions for the individual systems, and, for example, two similar molecules such as CO₂ and N₂O, which have nearly the same gas-phase rotational constant, have very different helium droplet rotational constants due to the differences in the interaction potentials [194]. Since inside helium droplets metastable structures can be formed, which may be impossible to be observed in the gas-phase, there is certainly a desire to be able to extract quantitative bond lengths and angles from the rotationally resolved spectra. Fully quantum mechanical calculations have been able to reproduce the experimentally determined rotational constants for a few prototype systems, which is certainly a first step [195–197]. Despite the ambiguity in rotational constants, the overall symmetry of the system is not affected, what can aid in structural determinations. Indeed the nuclear spin statistical weights for propargyl and all CH₃-HX-type complexes have confirmed the C_{2v} and C_{3v} symmetries of the isolated molecules, respectively.

As can be seen from previous reviews on the subject, almost all of our knowledge on the interaction of the droplet with a dopant has come from closed shell molecules. From the admittedly small group of open-shell molecules studied, which are all summarized in this review, we find that the interactions are generally the same for radicals. The biggest exception would be the fact that open shell alkali and the quasi closed shell heavier earth alkali metal atoms are not solvated by the droplets and instead reside on the surface, which generally results from a stronger He-He interaction than the corresponding He-metal interaction. It was first unclear as to whether the interaction with an open shell molecule would be favorable at all, i. e. whether the radical would go into the droplet, based on the known repulsive interaction between lone electrons and helium droplets. For open shell atoms in non-*S* states, i. e. halogen atoms (2P), the electrostatic interactions with the quadrupole moment of the atom are quite strong, thus in general allowing for solvation.

Even if the species goes into the droplet, a localized unpaired electron may cause density distortions of the surrounding helium, which could lower the overall symme-

try. Indeed such effects were postulated for NO, which would give rise to a first order splitting of the two parity components. In that light the different effects of the helium droplet environment on the parity splitting of bare NO and the NO-HF complex show how such effects depend on details of the molecular system and the molecule-helium interactions. Theoretical support is urgently needed to describe and understand these detailed experimental results.

VI. FUTURE DIRECTIONS

A. High energy structures for chemical energy storage

The possibilities to build metastable molecular cluster structures inside liquid helium nano-droplets was demonstrated, for example, by observing a ring of six water molecules [61] or by the self-assembly of long linear chains of HCN [60]. These chains are built up due to the specific kinetic control of the complex formation inside the helium droplets. Since individual molecules are picked up successively by the droplet and are rapidly cooled inside with a rate of $\sim 10^{16} \text{ K s}^{-1}$, they approach each other isothermally at low temperature (0.4 K). Already at relatively long distance the molecules are oriented in the field produced by the dipole of the complexation partner. The ground states are high-field seeking and therefore the molecular dipoles of both partners are oriented along the intermolecular axis while they approach each other. Once they are close to each other, they find themselves in a linear, hydrogen bonded geometry. Due to the low temperature they cannot rearrange to form the thermodynamically more stable cyclic structures observed in free jets [198, 199].

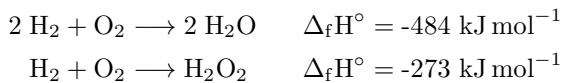
In the same way as for HCN it should be possible to assemble chains of polar radicals in helium droplets, e. g. chains of CN or OH radicals. Considering two ground-state OH radicals approaching one another from long range at very low temperatures, the hydrogen peroxide structure is the global minimum product. Nevertheless, there is also a hydrogen bonded minimum at long range analogous to the HF dimer [200, 201]. At long range the ground state OH-OH interactions are essentially the same as for the HF dimer. Since the length scale for the hydrogen-bond is very different from that of the chemical well, it is expected that after reaching the hydrogen-bonded well there is a barrier to further bond-compression, before the O-O distance is decreased sufficiently to access the chemical bonding region. In systems with such barriers the possibility exists for stabilizing the pre-reactive complex in the hydrogen bonded well inside a helium droplet, in analogy to the physisorbed state in surface science. The challenge is to remove the condensation energy from the system as it forms, before it can sur-

mount any barriers, thus trapping it in the pre-reactive form. The natural extension to larger OH clusters suggests that one might be able to make a whole new class of pre-reactive radical solids.

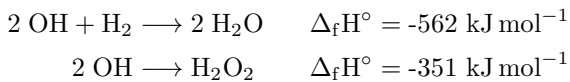
The qualitative description given above is supported by extensive theoretical studies of the hydrogen peroxide system. Particularly interesting is a high-level theoretical study by Kuhn *et al.*, in which a minimum energy path analysis shows how the bonding character changes from long range hydrogen bonding to covalent bonding at decreased O–O distances [202]. These two regions are separated by a significant barrier – some hundred wavenumbers for the highest quality potential – that is presumably high enough to exhibit bound states in the hydrogen bonded well. Moreover, the minimum energy path from these calculations shows a cusp at the maximum of the barrier, corresponding to a sudden change in the angular geometry of the complex at that distance. This is due to the need for switching from a geometry with the molecular dipoles oriented parallel (OH–OH) to an head-to-head structure (HO–OH).

With this theoretical work supporting the existence of a barrier between the hydrogen bonded and the chemically bonded minima, there is good reason to think that the pre-reactive dimer, as well as larger nanoclusters, can be stabilized by following the minimum energy approach path analogous to the production of HCN chains [60], cyclic water hexamer [61], and polymers of HF [203–206]. $(H_2)_n$ -HF clusters, which are a good model for the OH/H₂ metastable system, have also been studied in helium droplets [207–210]. These studies show that there is considerable control on the number of molecules picked up by the droplets, allowing the study of a wide range of stoichiometries. Generally, supermolecular structures with large dipoles are favored by the formation process. It has to be pointed out that all systems mentioned form different, metastable, structures in liquid helium droplets, than obtained from gas-phase nucleation. The implication is that liquid helium provides a new growth medium for creating and stabilizing higher energy isomers of clusters that are not normally observed in the gas-phase. It is also encouraging that different clusters of quite large size using can be differentiated using infrared pendular state spectroscopy [60].

To illustrate what might be achieved by producing analogous metastable structures of radicals, consider the hydrogen-oxygen reactions [211–213]:



and for comparison, consider the following reactions:



Thus, if solids of pure OH or with a OH/H₂ ration of 2:1

could be stabilized, these would exhibit exothermicities that are considerably higher than that of the hydrogen-oxygen system, which is widely used as fuel. As such they would be ideal combustibles for high energy consumptions. From the discussion given above, there is plenty of evidence to suggest this could be achieved, both in nano-droplets and in bulk helium.

Other systems that could potentially provide an even larger amount of chemical energy storage are nitrogen (oxygen) oligomers, which react very exothermally to form stable N₂ (O₂) molecules. The N₃ and N₄ molecules have been predicted [214–216] and observed experimentally [217, 218]. The cluster formation mechanism in helium droplets described above should allow one to produce a wide variety of such metastable N_n systems from nitrogen atoms, where n could be much larger than 3 and is solely determined by the N-atom density in the pick-up region.

Gordon and co-workers have shown that similar radical solids can be stabilized in bulk liquid helium.[247] They directed a helium beam containing atomic nitrogen into a dewar of liquid helium, to find that a highly energetic, snow-like precipitate was formed [219–221]. Upon warming that material thermally detonated. Electron spin measurements have shown an unexpectedly high concentration of N atoms with more than 10 % of the N₂ concentration in the original experiments. Later the experiments were optimized to obtain atomic concentrations as high as 50 % [222]. Although a number of techniques have been used to study the properties of these cryo-solids, detailed structural information is still lacking. Nevertheless the authors point out that the liquid helium is only necessary during the formation process and have shown that the resulting solids are stable when the liquid helium is completely evaporated, as long as the temperature remains below approximately 8 K [220]. Most remarkably the authors were able to use a plunger to compact the solid precipitate into a pellet without causing it to react [223]. They suggest that the method should be applicable to a wide range of species and we suspect that it will be even more effective for *molecular* radicals, where there are steric considerations that also inhibit recombination. A number of fascinating observations have been made by this group, including the appearance of an *intense green glow* when the sample was irradiated with an helium neon laser. More recently they showed that captured N(²D) atoms show thermoluminescence upon slight heating by 0.1 K or when irradiating them using microwaves [224, 225]. Details of the impurity condensation in liquid and solid helium and the interpretation of their X-ray and IR spectroscopic studies have recently been discussed [226].

Structural information on such materials is clearly desirable and can be obtained from vibrational spectroscopy on small (nanoscale) samples of these materials. Studies in liquid helium droplets will provide better control of the growth, as well as the ability to use high resolution vi-

brational and rotational spectroscopy to characterize the resulting structures. For smaller clusters rotational resolution will be possible, providing detailed information on the corresponding structures.

The nanosolids we are proposing to make in these studies are highly energetic and it is interesting to consider what will happen when they are vibrationally excited. If the vibrational energy deposited in the molecules is sufficient to overcome the barriers that are responsible for the stability of the clusters, and the energy becomes redistributed into the reaction coordinate by intramolecular vibrational energy redistribution (IVR), it is expected to observe strong responses to the laser excitation. This laser-induced detonation (LID) will result in complete evaporation of the helium droplet resulting in very strong depletion signals. Alternatively, the clusters might dissipate the vibrational energy to the helium so quickly that no reaction does occur and the system simply cools back down by evaporation of liquid helium atoms. These effects could be studied using IR-IR pump-probe experiments, similar to the ones demonstrated for stable species embedded in helium droplets [62, 63]. Considering the OH-OH system, it is interesting to consider excitation of the OH-OH intermolecular vibrations, i. e. using combination modes of this vibration. This will put energy into the reaction coordinate and may push the system over the barrier and into the reactive well. Such tests of the stability of these solid materials are important in accessing the usefulness of such materials as specialty fuels. Understanding the growth of such new classes of high energy density materials in liquid helium can be used to make and study the properties and structures of these systems on the nanometer scale. What is exciting about this approach is that it has the potential to be scaled up to macroscopic sizes, as demonstrated by the experiments of Gordon and co-workers [219–222].

Considering the Br-HCN and HCN-Br complexes described above, it seems reasonable to allow for the formation of a metastable Br-HCN-Br complex as such a high-energy structure. Whereas we were not able to find this HCN complex, first experiments using the equivalent cyanoacetylene (HCCCN) chromophore reveal the existence of such complexes. In Figure 12 pendular survey scans for the bromine-cyanoacetylene system are shown for different experimental conditions. It is important to note that scans 12(A) - (C) were recorded by picking up the HCCCN first, but in 12(D) the order has been reversed, and we instead pick-up from the pyrolysis source first. In scan 12(A), only HCCCN is added to the droplets, while in 12(B), Br₂ is flowing through a room temperature pyrolysis source. The result of heating the pyrolysis to the appropriate temperatures for bromine atom pick-up are shown in scans 12(C) and (D). In good agreement with the results of X + HCN, we find two peaks at 3326.1 and 3302.4 cm⁻¹, marked by a †, which we assign to the Br-HCCCN and HCCCN-Br complexes, respectively, based on their frequency shifts and signal

strengths. The peaks labeled with an * were found to optimize at higher HCCCN pressure, therefore they correspond to complexes containing more than one HCCCN. The peak at 3297.65 cm⁻¹ optimizes at the same HCCCN pressure as the 1:1 complexes, however, it is found to optimize at higher bromine pressure, suggesting that it is a complex containing two bromine atoms [123, 158]. Since it only appears in the spectrum when the HCCCN is picked up first, it is a good candidate for being Br-HCCCN-Br, a metastable van der Waals complex containing two spatially separated bromine atoms. The dependence on pick-up order is to be expected because two bromine atoms will likely recombine to form Br₂ in the absence of the molecular spacer.

To aid in this preliminary assignment we performed bromine pressure dependence measurements [123]. This new peak is found to optimize at higher bromine pressures than those peaks assigned to the 1:1 complexes, and agrees well with a simulation of a dimer using a Poisson distribution for the pick-up statistics. Although we cannot rule out that a Br-HCCCN-Br₂, or similar complex might have such a pick-up cell pressure dependence, a double-resonance population transfer experiment [63] in which this new peak is pumped and the HCCCN-Br₂ complex is recovered would be definitive.

It is also interesting to note, that the the original interest in stabilizing spin-polarized hydrogen arose because

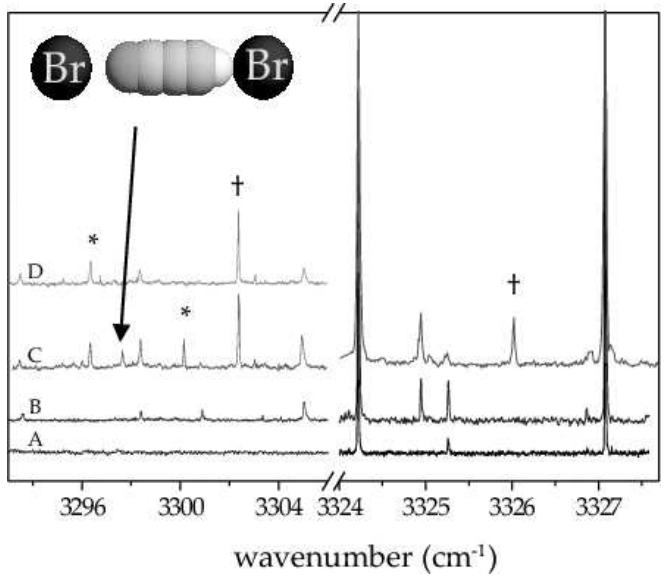


Figure 12: Pendular survey scans for the Br + HCCCN system, where the bromine pressure is intentionally high to facilitate forming larger clusters. In (A) only HCCCN is picked up by the droplets and in (B) Br₂ is flowing through the cold pyrolysis source. Scans (C) and (D) were both recorded with the pyrolysis source at the appropriate temperature for bromine atom production. Whereas in (C) the HCCCN is picked up first, in (D) the bromine atoms are picked up first. See text for details.

of the same reasons, namely searching for novel high-energy structures [227–229]. The reaction $H + H \rightarrow H_2$ is exothermic by more than 400 kJ cm^{-1} , yielding a very large energy-to-mass ratio if samples of atomic hydrogen could be stabilized. For two polarized hydrogen atoms direct molecule formation is not possible, as their $^3\Sigma_u^+$ potential is purely repulsive, and a spin-flip is necessary for the binding energy of the hydrogen molecule to be released. Whereas the preparation of dense samples of spin-polarized hydrogen for energy storage has not been successful yet, these studies emerged into the quest for the experimental realization of Bose-Einstein condensation and yielded a whole new field in atomic and molecular physics [230, 231]. Nowadays similar ideas are also discussed in the context of deep space propulsion systems based on antihydrogen [232].

B. Other applications

Recently a new experiment for a sensitive search for the electric dipole moment (EDM) of the electron using matrix-isolated dipolar radicals was proposed [233]. It was suggested to measure the magnetization of an oriented sample of diatomic radicals embedded in a solid noble-gas matrix. While the solid state matrix will provide a larger number density of radicals, it is not clear to what degree molecular orientation can be achieved, since neither the break-down voltages of the matrix nor the details of the cage effects in the matrix sites are known [233]. As shown for several examples in this review, pendular states with a high degree of orientation can easily be achieved for polar molecules embedded in liquid helium droplet. Therefore, the techniques of strong field orientation of radicals embedded in liquid helium droplets, as described in this review, might provide a well-defined environment for sensitive EDM tests.

The OH radical receives also considerable attention in the field of ultracold polar molecules and it has been successfully confined in electrostatic traps for times $> 1 \text{ s}$ and at temperatures of $\sim 50 \text{ mK}$ [28, 234], and there is considerable interest to cool such trapped molecules further down to even lower temperatures. In that context the interaction of two OH molecules at very long range has been considered and for two rotational ground state OH radicals in their low-field seeking state, so-called *field-linked* states have been predicted: bound states of long-range OH-OH dipole aligned dimers that are stabilized by an external electric field on the order of 10 kV/cm [235]. Such field linked states provide a similar degree of control over the chemical reaction as the van der Waals-dimers described above. As long as the field is on, they are safely separated by several nanometers in their long-range well, but when the field is ramped down they can react — assuming that, for example, the exothermic reaction $2 \text{OH} \rightarrow \text{H}_2\text{O} + \text{O}$ proceeds at ultracold temperatures [235]. However, a gas of OH radicals in low-field seeking states is

subject to large collisional losses and is therefore not suitable for evaporative cooling [236]. The high-field seeking state is collisionally stable, being the lowest energy state of OH, however, it does not show such long-range states and the collisional parameters are strongly depending on the short-range potential and must be determined by a “suitable experiment” [235]. Experiments on entrance-channel complexes in helium droplets, like the ones described in this paper, would provide detailed information on this PES.[248]

C. Experimental improvements

The main hurdle for studying transient species embedded in superfluid helium droplets is the generation of the necessary clean samples of radicals. Albeit the continuous pyrolysis source [67] proves to be a very successful and versatile tool for the production of a wide range of radicals, the types of radicals that can be produced is still quite limited. It seems impossible, for example, to use it to create clean sources of oxygen or nitrogen atoms, as necessary for the experiments proposed above, as that would require to thermally break the extremely strong O_2 or N_2 bonds.

Alternative techniques that have been used so successfully in free jet experiments, such as photolysis or discharge sources, can not easily be coupled to the continuous droplet beam setups, which up to date in the vast majority are operated in a cw fashion. Once pulsed droplet beams mature they will provide much larger droplet densities, what might allow to couple them to pulsed radical sources. Nevertheless, the droplet property of embedding any species in the scattering region requires extremely clean sources that would still need to be developed, but the possibility of using photodissociation should help considerably to break strong bonds.

It would be extremely interesting to perform time-resolved studies on the processes of molecules embedded in helium droplets in order to study reactions and relaxation dynamics in real time. Femtosecond pump-probe experiments on alkali-doped helium droplets [237–239] show the feasibility of such experiments. In these experiments the dynamics of the helium-alkali atom interaction could clearly be observed. In a similar way it should be possible to observe relaxation dynamics after vibrational excitation of molecules like HCN embedded *inside* the helium droplets. Once metastable radical complexes, as described above, can be produced inside the helium droplets one could even photoinitiate their reaction and follow the complete chemical dynamics from the educts to the final products due to the confining environment of the droplets.

VII. SUMMARY

Superfluid helium droplets provide a novel medium for the study of transient and reactive species. A continuous pyrolysis source to produce extremely clean, effusive beams of radicals suitable for pick-up by helium droplet beams was developed and the radicals embedded in helium droplets were studied using high-resolution infrared spectroscopy. Using this setup, halogen atoms and hydrocarbon radicals were produced and their van der Waals complexes with HF or HCN were studied. In related studies NO and also a few other transient molecules were studied as well. Many of the systems studied provide new, detailed information on stationary points of PES that were previously only studied using reactive scattering experiments. Even further information and the possibility for optically controlled chemistry can be obtained using double-resonance techniques.

The results from these studies also provide a very sensitive probe of the quantum fluid the helium droplet environment provides, due to the influence of the droplet not only on the inertial parameters, as for closed shell molecules, but also on the electronic properties, as manifested in parity splitting or Λ -doubling parameters.

The ability to design complexes of multiple, potentially different stable and transient species inside these cryo-reactors promises a wide variety of possibilities, from studying stationary points on the PES of these reactive species, developing novel high-energy species, studying reaction dynamics under cold and defined conditions, to

optically induced chemical reactions.

However, the extraction of quantitative structural data from high-resolution spectra of molecules embedded in helium droplets is still quite limited, due to missing accurate models for the molecule-helium droplet interaction. However, there are progresses in the theoretical descriptions of these effects and they might once allow to determine accurate structural information, i. e. geometric rotational constants for the isolated molecular system from helium droplet experiments.

Acknowledgments

Most of the experimental work described herein was performed at the University of North Carolina at Chapel Hill in the group of Roger E. Miller, who deceased on 6. November 2005. The authors are very grateful for the opportunity to work with him and for the stimulating environment and support he provided to his group.

J. M. M. thanks Tom Baer for supporting him during the final stage of his graduate work. We thank Ad van der Avoird for providing the potential energy surfaces in Figure 3.

Financial support by NSF and AFOSR is acknowledged. J. K. gratefully acknowledges a Feodor Lynen fellowship of the Alexander von Humboldt Foundation and J. M. M. a scholarship by the Max Planck Society.

- [1] M. Y. Choi, G. E. Doublerly, T. M. Falconer, W. K. Lewis, C. M. Lindsay, J. M. Merritt, P. L. Stiles, and R. E. Miller, *Int. Rev. Phys. Chem.* **25**, 15 (2006).
- [2] F. Stienkemeier and K. K. Lehmann, *J. Phys. B* **39**, R127 (2006).
- [3] J. P. Toennies and A. F. Vilesov, *Angew. Chem. Int. Ed.* **43**, 2622 (2004).
- [4] G. N. Makarov, *Physics-Uspekhi* **47**, 217 (2004).
- [5] J. A. Northby, *J. Chem. Phys.* **115**, 10065 (2001).
- [6] C. Callegari, K. K. Lehmann, R. Schmied, and G. Scoles, *J. Chem. Phys.* **115**, 10090 (2001).
- [7] F. Stienkemeier and A. F. Vilesov, *J. Chem. Phys.* **115**, 10119 (2001).
- [8] J. Warnatz, U. Maas, and W. Dibble, *Combustion: Physical and Chemical Fundamentals, Modeling and Simulation, Experiments: Pollutant Formation* (Springer, Berlin, 1996).
- [9] R. P. Wayne, *Chemistry of Atmospheres: An introduction to the Chemistry of the Atmospheres of Earth, the Planets, and their satellites* (Oxford University Press, Oxford, GB, 1991), 2nd ed.
- [10] D. Chastaing, P. L. James, I. R. Sims, and I. W. M. Smith, *Phys. Chem. Chem. Phys.* **1**, 2247 (1999).
- [11] J. H. Van't Hoff, *Études de dynamique chimique* (Muller, Amsterdam, 1884).
- [12] S. Arrhenius, *Z. Phys. Chem.* **4**, 226 (1889).
- [13] F. London, *Zeitschrift für Elektrochemie und Angewandte Physikalische Chemie* **35**, 552 (1929).
- [14] H. Eyring and M. Polanyi, *Z. Phys. Chem. B* **12**, 279 (1931).
- [15] G. S. Hammond, *J. Am. Chem. Soc.* **77**, 334 (1955).
- [16] J. C. Polanyi and W. H. Wong, *J. Chem. Phys.* **51**, 1439 (1969).
- [17] M. H. Qiu, Z. F. Ren, L. Che, D. X. Dai, S. A. Harich, X. Y. Wang, X. M. Yang, C. X. Xu, D. Q. Xie, M. Gustafsson, et al., *Science* **311**, 1440 (2006).
- [18] S. D. Chao, S. A. Harich, D. X. Dai, C. C. Wang, X. M. Yang, and R. T. Skodje, *J. Chem. Phys.* **117**, 8341 (2002).
- [19] J. Y. Zhang, D. X. Dai, C. C. Wang, S. A. Harich, X. Y. Wang, X. M. Yang, M. Gustafsson, and R. T. Skodje, *Phys. Rev. Lett.* **96**, 093201 (2006).
- [20] J. J. Valentini, *Ann. Rev. Phys. Chem.* **52**, 15 (2001).
- [21] D. H. Parker and R. B. Bernstein, *Ann. Rev. Phys. Chem.* **40**, 561 (1989).
- [22] H. J. Loesch, *Ann. Rev. Phys. Chem.* **46**, 555 (1995).
- [23] A. J. OrrEwing, *J. Chem. Soc. – Faraday Trans.* **92**, 881 (1996).
- [24] P. Casavecchia, *Rep. Prog. Phys.* **63**, 355 (2000).
- [25] H. L. Bethlem, M. R. Tarbutt, J. Küpper, D. Carty,

K. Wohlfart, E. A. Hinds, and G. Meijer, *J. Phys. B* **39**, R263 (2006).

[26] H. L. Bethlem, G. Berden, and G. Meijer, *Phys. Rev. Lett.* **83**, 1558 (1999).

[27] H. L. Bethlem and G. Meijer, *Int. Rev. Phys. Chem.* **22**, 73 (2003).

[28] S. Y. T. van de Meerakker, N. Vanhaecke, and G. Meijer, *Ann. Rev. Phys. Chem.* **57**, 159 (2006).

[29] C. E. Heiner, H. L. Bethlem, and G. Meijer, *Phys. Chem. Chem. Phys.* **8**, 2666 (2006).

[30] J. J. Gilijamse, S. Hoekstra, S. Y. T. van de Meerakker, G. C. Groeneboom, and G. Meijer, *Science* (2006), accepted for publication.

[31] H. J. Werner, W. Bian, M. Menendez, F. J. Aoiz, P. Casavecchia, L. Cartechini, and N. Balucani, *Chem. Phys. Lett.* **328**, 500 (2000).

[32] N. Balakrishnan, *J. Chem. Phys.* **121**, 5563 (2004).

[33] D. Skouteris, D. E. Manolopoulos, W. Bian, H. J. Werner, L. H. Lai, and K. Liu, *Science* **286**, 1713 (1999).

[34] H. J. Werner, W. Bian, and U. Manthe, *Chem. Phys. Lett.* **313**, 647 (1999).

[35] P. F. Weck and N. Balakrishnan, *Int. Rev. Phys. Chem.* **25**, 283 (2006).

[36] D. Townsend, S. A. Lahankar, S. K. Lee, S. D. Chambreau, A. G. Suits, X. Zhang, J. Rheinecker, L. B. Harding, and J. M. Bowman, *Science* **306**, 1158 (2004).

[37] S. D. Chambreau, D. Townsend, S. A. Lahankar, S. K. Lee, and A. G. Suits, *Physica Scripta* **73**, C89 (2006).

[38] C. Murray and A. J. Orr-Ewing, *Int. Rev. Phys. Chem.* **23**, 435 (2004).

[39] M. C. Heaven, *Int. Rev. Phys. Chem.* **24**, 375 (2005).

[40] Y. Kim and H. Meyer, *Int. Rev. Phys. Chem.* **20**, 219 (2001).

[41] M. I. Lester, B. V. Pond, M. D. Marshall, D. T. Anderson, L. B. Harding, and A. F. Wagner, *Faraday Disc.* **118**, 373 (2001).

[42] R. A. Loomis, R. L. Schwartz, and M. I. Lester, *J. Chem. Phys.* **104**, 6984 (1996).

[43] D. T. Anderson, R. L. Schwartz, M. W. Todd, and M. I. Lester, *J. Chem. Phys.* **109**, 3461 (1998).

[44] R. A. Loomis and M. I. Lester, *Ann. Rev. Phys. Chem.* **48**, 643 (1997).

[45] R. L. Schwartz, D. T. Anderson, M. W. Todd, and M. I. Lester, *Chem. Phys. Lett.* **273**, 18 (1997).

[46] J. M. Hossenlopp, D. T. Anderson, M. W. Todd, and M. I. Lester, *J. Chem. Phys.* **109**, 10707 (1998).

[47] Y. L. Chen and M. C. Heaven, *J. Chem. Phys.* **109**, 5171 (1998).

[48] A. L. Kaledin and M. C. Heaven, *Chem. Phys. Lett.* **347**, 199 (2001).

[49] Y. L. Chen and M. C. Heaven, *J. Chem. Phys.* **112**, 7416 (2000).

[50] M. D. Wheeler, D. T. Anderson, and M. I. Lester, *Int. Rev. Phys. Chem.* **19**, 501 (2000).

[51] Z. Mielke and L. Andrews, *J. Phys. Chem.* **94**, 3519 (1990).

[52] M. E. Jacox, *Chem. Phys.* **42**, 133 (1979).

[53] L. Khriachtchev, H. Tanskanen, and M. Rasanen, *J. Chem. Phys.* **124**, 181101 (2006).

[54] K. Yoshioka, P. L. Raston, and D. T. Anderson, *Int. Rev. Phys. Chem.* **25**, 469 (2006).

[55] T. Momose, H. Hoshina, M. Fushitani, and H. Katsuki, *Vibrational Spectroscopy* **34**, 95 (2004).

[56] T. Momose, M. Fushitani, and H. Hoshina, *Int. Rev. Phys. Chem.* **24**, 533 (2005).

[57] T. Momose, H. Hoshina, N. Sogoshi, H. Katsuki, T. Wakabayashi, and T. Shida, *J. Chem. Phys.* **108**, 7334 (1998).

[58] S. Grebenev, J. P. Toennies, and A. F. Vilesov, *Science* **279**, 2083 (1998).

[59] M. Hartmann, R. E. Miller, J. P. Toennies, and A. F. Vilesov, *Phys. Rev. Lett.* **75**, 1566 (1995).

[60] K. Nauta and R. E. Miller, *Science* **283**, 1895 (1999).

[61] K. Nauta and R. E. Miller, *Science* **287**, 293 (2000).

[62] J. M. Merritt, G. E. Douberly, and R. E. Miller, *J. Chem. Phys.* **121**, 1309 (2004).

[63] G. E. Douberly, J. M. Merritt, and R. E. Miller, *Phys. Chem. Chem. Phys.* **7**, 463 (2005).

[64] D. M. Brink and S. Stringari, *Z. Phys. D* **15**, 257 (1990).

[65] F. Dalfovo and S. Stringari, *J. Chem. Phys.* **115**, 1078 (2001).

[66] K. K. Lehmann, *J. Chem. Phys.* **119**, 3336 (2003).

[67] J. Küpper, J. M. Merritt, and R. E. Miller, *J. Chem. Phys.* **117**, 647 (2002).

[68] P. A. Block, E. J. Bohac, and R. E. Miller, *Phys. Rev. Lett.* **68**, 1303 (1992).

[69] E. W. Becker, R. Klingelhofer, and P. Lohse, *Z. Naturforsch. A* **16**, 1259 (1961).

[70] K. Nauta and R. E. Miller, *J. Chem. Phys.* **115**, 10138 (2001).

[71] K. von Haeften, A. Metzelthin, S. Rudolph, V. Staemmler, and M. Havenith, *Phys. Rev. Lett.* **95**, 215301 (2005).

[72] H. Pauly, in [240], chap. 4, pp. 83–123.

[73] H. Pauly, in [240], chap. 5, pp. 124–152.

[74] D. W. Kohn, H. Clauberg, and P. Chen, *Rev. Sci. Instrum.* **63**, 4003 (1992).

[75] M. R. Cameron and S. H. Kable, *Rev. Sci. Instrum.* **67**, 283 (1996).

[76] X. Zhang, A. V. Friderichsen, S. Nandi, G. B. Ellison, D. E. David, J. T. McKinnon, T. G. Lindeman, D. C. Dayton, and M. R. Nimlos, *Rev. Sci. Instrum.* **74**, 3077 (2003).

[77] P. C. Engelking, *Rev. Sci. Instrum.* **57**, 2274 (1986).

[78] P. C. Engelking, *Chem. Rev.* **91**, 399 (1991).

[79] D. T. Anderson, S. Davis, T. S. Zwier, and D. J. Nesbitt, *Chem. Phys. Lett.* **258**, 207 (1996).

[80] D. L. Monts, T. G. Dietz, M. A. Duncan, and R. E. Smalley, *Chem. Phys.* **45**, 133 (1980).

[81] M. Heaven, T. A. Miller, and V. E. Bondybey, *Chem. Phys. Lett.* **84**, 1 (1981).

[82] P. Andresen, D. Hausler, and H. W. Lulf, *J. Chem. Phys.* **81**, 571 (1984).

[83] M. N. Slipchenko, S. Kuma, T. Momose, and A. F. Vilesov, *Rev. Sci. Instrum.* **73**, 3600 (2002).

[84] S. Yang, S. M. Brereton, and A. M. Ellis, *Rev. Sci. Instrum.* **76**, 104102 (2005).

[85] A. Conjusteau, Ph.D. thesis, Princeton University, Princeton, NJ, USA (2002).

[86] A. Braun and M. Drabbels, *Phys. Rev. Lett.* **93**, 253401 (2004).

[87] K. Kavita and P. K. Das, *J. Chem. Phys.* **112**, 8426 (2000).

[88] D. H. Parker and A. Eppink, *J. Chem. Phys.* **107**, 2357 (1997).

[89] M. Fárník and J. P. Toennies, *J. Chem. Phys.* **122**, 014307 (2005).

[90] W. K. Lewis, C. M. Lindsay, R. J. Bemish, and R. E.

Miller, J. Am. Chem. Soc. **127**, 7235 (2005).

[91] N. M. Marinov, W. J. Pitz, C. K. Westbrook, A. M. Vincitore, M. J. Castaldi, S. M. Senkan, and C. F. Melius, Combust. Flame **114**, 192 (1998).

[92] P. R. Westmoreland, A. M. Dean, J. B. Howard, and J. P. Longwell, J. Phys. Chem. **93**, 8171 (1989).

[93] U. Alkemade and K. H. Homann, Z. Phys. Chem. **161**, 19 (1989).

[94] S. E. Stein, J. A. Walker, M. M. Suryan, and A. Fahr, in *Symp. (Int.) Combust.* (1990), vol. 23, pp. 85–90.

[95] P. Botschwina, R. Oswald, J. Flügge, and M. Horn, Z. Phys. Chem. **188**, 29 (1995).

[96] P. Botschwina, M. Horn, R. Oswald, and S. Schmatz, J. Electron. Spectrosc. **108**, 109 (2000).

[97] H. Honjou, M. Yoshimine, and J. Pacansky, J. Phys. Chem. **91**, 4455 (1987).

[98] A. Hinchcliffe, J. Mol. Struct. **37**, 295 (1977).

[99] C. H. Wu and R. D. Kern, J. Phys. Chem. **91**, 6291 (1987).

[100] N. M. Marinov, M. J. Castaldi, C. F. Melius, and W. Tsang, Combust. Sci. Technol. **128**, 295 (1997).

[101] I. Glassman, in *Symp. (Int.) Combust.* (1988), vol. 22, p. 295.

[102] J. A. Miller, in *Symp. (Int.) Combust.* (1996), vol. 26, p. 461.

[103] J. M. Goodings, D. K. Bohme, and C.-W. Ng, Combust. Flame **36**, 27 (1979).

[104] D. B. Olson and H. F. Calcote, in *Symp. (Int.) Combust.* (1981), vol. 18, p. 453.

[105] K. Tanaka, T. Harada, K. Sakaguchi, K. Harada, and T. Tanaka, J. Chem. Phys. **103**, 6450 (1995).

[106] L. Yuan, J. DeSain, and R. F. Curl, J. Mol. Spec. **187**, 102 (1998).

[107] K. Tanaka, Y. Sumiyoshi, Y. Ohshima, Y. Endo, and K. Kawaguchi, J. Chem. Phys. **107**, 2728 (1997).

[108] P. L. Chrapovsky and L. J. F. Hermans, Ann. Rev. Phys. Chem. **50**, 315 (1999).

[109] M. Fushitani and T. Momose, J. Chem. Phys. **116**, 10739 (2002).

[110] P. L. Stiles, K. Nauta, and R. E. Miller, Phys. Rev. Lett. **90**, 135301 (2003).

[111] P. Botschwina, *The zero-point corrected dipole moment of propargyl radical* (2002), private communication.

[112] C. M. Lindsay, W. K. Lewis, and R. E. Miller, J. Chem. Phys. **121**, 6095 (2004).

[113] K. Nauta and R. E. Miller, J. Chem. Phys. **113**, 9466 (2000).

[114] E. Polyakova, D. Stolyarov, and C. Wittig, J. Chem. Phys. **124**, 214308 (2006).

[115] F. Stienkemeier, J. Higgins, W. E. Ernst, and G. Scoles, Z. Phys. B **98**, 413 (1995).

[116] J. Reho, C. Callegari, J. Higgins, W. E. Ernst, K. K. Lehmann, and G. Scoles, Faraday Disc. **108**, 161 (1997).

[117] F. R. Brühl, R. A. Trasca, and W. E. Ernst, J. Chem. Phys. **115**, 10220 (2001).

[118] E. Lugovoj, J. P. Toennies, and A. Vilesov, The Journal of Chemical Physics **112**, 8217 (2000).

[119] E. Herbst and K. W., Astron. J. **185**, 505 (1973).

[120] D. Smith, Chem. Rev. **92**, 1473 (1992).

[121] D. M. Neumark, Phys. Chem. Comm **5**, 76 (2002).

[122] A. J. C. Varandas, P. J. S. B. Caridade, J. Z. H. Zhang, Q. Cui, and K. L. Han, J. Chem. Phys. **125**, 064312 (2006).

[123] J. M. Merritt, J. Küpper, and R. E. Miller, Phys. Chem. Chem. Phys. (2006), submitted.

[124] J. M. Merritt, J. Küpper, and R. E. Miller, Phys. Chem. Chem. Phys. **7**, 67 (2005).

[125] M. L. Dubernet and J. M. Hutson, J. Chem. Phys. **101**, 1939 (1994).

[126] C. S. Maierle, G. C. Schatz, M. S. Gordon, P. McCabe, and J. N. Connor, J. Chem. Soc. – Faraday Trans. **93**, 709 (1997).

[127] P. Jungwirth, P. Zdanska, and B. Schmidt, J. Phys. Chem. A **102**, 7241 (1998).

[128] M. Bittererova and S. Biskupic, Chem. Phys. Lett. **299**, 145 (1999).

[129] M. Meuwly and J. M. Hutson, Phys. Chem. Chem. Phys. **2**, 441 (2000).

[130] M. Meuwly and J. M. Hutson, J. Chem. Phys. **112**, 592 (2000).

[131] M. Meuwly and J. M. Hutson, J. Chem. Phys. **119**, 8873 (2003).

[132] J. A. Kłos, G. Chałasiński, M. M. Szczęśniak, and H.-J. Werner, J. Chem. Phys. **115**, 3085 (2001).

[133] W. B. Zeimen, J. A. Kłos, G. C. Groenenboom, and A. van der Avoird, J. Phys. Chem. A **107**, 5110 (2003), see erratum: [241].

[134] D. M. Neumark, Ann. Rev. Phys. Chem. **43**, 153 (1992).

[135] M. P. Deskevich, M. Y. Hayes, K. Takahashi, R. T. Skodje, and D. J. Nesbitt, J. Chem. Phys. **124**, 224303 (2006).

[136] A. V. Fishchuk, P. E. S. Wormer, and A. van der Avoird, Journal Of Physical Chemistry A **110**, 5273 (2006).

[137] A. V. Fishchuk, G. C. Groenenboom, and A. van der Avoird, Journal Of Physical Chemistry A **110**, 5280 (2006).

[138] M. L. Dubernet and J. Hutson, J. Phys. Chem. **98**, 5844 (1994).

[139] K. Liu, A. Kolessov, J. W. Partin, I. Bezel, and C. Wittig, Chem. Phys. Lett. **299**, 374 (1999).

[140] K. Imura, H. Ohoyama, R. Naaman, D. C. Che, M. Hashinokuchi, and T. Kasai, J. Mol. Struct. **552**, 137 (2000).

[141] J. M. Mestdagh, B. Soep, M. A. Gaveau, and J. P. Visitot, Int. Rev. Phys. Chem. **22**, 285 (2003).

[142] L. Andrews and R. D. Hunt, J. Chem. Phys. **89**, 3502 (1988).

[143] R. D. Hunt and L. Andrews, J. Chem. Phys. **88**, 3599 (1988).

[144] R. D. Hunt and L. Andrews, J. Phys. Chem. **92**, 3769 (1988).

[145] A. M. G. Ding, L. J. Kirsch, D. S. Perry, J. C. Polanyi, and J. L. Schreiber, Faraday Disc. Chem. Soc **55**, 252 (1973).

[146] E. Würzberg, A. J. Grimley, and P. L. Houston, Chem. Phys. Lett. **57**, 373 (1978).

[147] E. Würzberg and P. L. Houston, J. Chem. Phys. **72**, 5915 (1980).

[148] C. M. Moore, I. W. M. Smith, and D. W. A. Stewart, Int. J. Chem. Kin. **26**, 813 (1994).

[149] K. Tamagake, D. W. Setser, and J. P. Sung, J. Chem. Phys. **73**, 2203 (1980).

[150] A. Zolot and D. J. Nesbitt, manuscript in preparation.

[151] R. B. Metz, J. M. Pfeiffer, J. D. Thoemke, and F. F. Crim, Chem. Phys. Lett. **221**, 347 (1994).

[152] C. Kreher, R. Theinl, and K. H. Gericke, J. Chem. Phys. **104**, 4481 (1996).

[153] B. K. Decker, G. He, I. Tokue, and R. G. Macdonald,

J. Phys. Chem. A **105**, 5759 (2001).

[154] M. Y. Hayes, M. P. Deskevich, D. J. Nesbitt, K. Takahashi, and R. T. Skodje, J. Phys. Chem. A **110**, 436 (2006).

[155] O. D. Krogh and G. C. Pimentel, J. Chem. Phys. **67**, 2993 (1977).

[156] H. J. Loesch and A. Remscheid, J. Chem. Phys. **93**, 4779 (1990).

[157] J. M. Rost, J. C. Griffin, B. Friedrich, and D. R. Herschbach, Phys. Rev. Lett. **68**, 1299 (1992).

[158] J. M. Merritt, Ph.D. thesis, University of North Carolina at Chapel Hill, Chapel Hill, NC, USA (2006).

[159] R. D. Hunt and L. Andrews, Inorg. Chem. **26**, 3051 (1987).

[160] I. U. Goldschleger, A. V. Akimov, E. Y. Misochko, and C. A. Wight, Mendeleev Comm. pp. 43–45 (2001).

[161] K. Schneider, P. Kramper, S. Schiller, and J. Mlynek, Opt. Lett. **22**, 1293 (1997).

[162] M. van Herpen, S. te Lintel Hekkert, S. E. Bisson, and F. J. M. Harren, Opt. Lett. **27**, 640 (2002).

[163] J. M. Merritt and R. E. Miller, in preparation.

[164] G. E. Doublerly, P. L. Stiles, and R. E. Miller, to be published.

[165] G. E. Doublerly, Ph.D. thesis, University of North Carolina at Chapel Hill, Chapel Hill, NC, USA (2006).

[166] P. L. Stiles and R. E. Miller, J. Phys. Chem. A **110**, 5620 (2006).

[167] K. Nauta, D. T. Moore, P. L. Stiles, and R. E. Miller, Science **292**, 481 (2001).

[168] P. L. Stiles, D. T. Moore, and R. E. Miller, J. Chem. Phys. **121**, 3130 (2004).

[169] D. T. Moore and R. E. Miller, J. Phys. Chem. A **108**, 9908 (2004).

[170] F. Dong and R. E. Miller, J. Phys. Chem. A **108**, 2181 (2004).

[171] W. Shiu, J. J. Lin, and K. Liu, Phys. Rev. Lett. **92**, 103201 (2004).

[172] T. S. Chu, X. Zhang, L. P. Ju, L. Yao, K. L. Han, M. L. Wang, and J. Z. H. Zhang, Chem. Phys. Lett. **424**, 243 (2006).

[173] G. L. Johnson and L. Andrews, J. Am. Chem. Soc. **102**, 5736 (1980).

[174] E. Y. Misochko, V. A. Benderskii, A. U. Goldschleger, A. V. Akimov, and A. F. Shestakov, J. Am. Chem. Soc. **117**, 11997 (1995).

[175] E. Y. Misochko, V. A. Benderskii, A. U. Goldschleger, A. V. Akimov, A. V. Benderskii, and C. A. Wight, J. Chem. Phys. **106**, 3146 (1996).

[176] Z. Liu, H. Gomez, and D. M. Neumark, Chem. Phys. Lett. **332**, 65 (2000).

[177] S. Rudić, J. M. Merritt, and R. E. Miller, J. Chem. Phys. **124**, 104305 (2006).

[178] K. P. Liu, Ann. Rev. Phys. Chem. **52**, 139 (2001).

[179] T. Gilbert, T. L. Grebner, I. Fischer, and P. Chen, Journal Of Chemical Physics **110**, 5485 (1999).

[180] L. Castiglioni, A. Bach, and P. Chen, J. Phys. Chem. A **109**, 962 (2005).

[181] S. J. Blanksby and G. B. Ellison, Acct. Chem. Res. **36**, 255 (2003).

[182] H. J. Curran, P. Gaffuri, W. J. Pitz, and C. K. Westbrook, Combust. Flame **114**, 149 (1998).

[183] O. J. Nielsen and T. J. Wallington, *Ultraviolet Absorption Spectra of Peroxy Radicals in the Gas Phase* (John Wiley & Sons, New York, NY, USA, 1997), pp. 72–73.

[184] M. B. Pushkarsky, S. J. Zalyubovsky, and T. A. Miller, J. Chem. Phys. **112**, 10695 (2000).

[185] S. J. Zalyubovsky, B. G. Glover, and T. A. Miller, J. Phys. Chem. A **107**, 7704 (2003).

[186] S. J. Zalyubovsky, B. G. Glover, T. A. Miller, C. Hayes, J. K. Merle, and C. M. Hadad, J. Phys. Chem. A **109**, 1308 (2005).

[187] B. G. Glover and T. A. Miller, J. Phys. Chem. A **109**, 11191 (2005).

[188] G. Tarczay, S. J. Zalyubovsky, and T. A. Miller, Chem. Phys. Lett. **406**, 81 (2005).

[189] J. Rienstra-Kiracofe, W. Allen, and H. Schaefer, III, J. Phys. Chem. A **104**, 9823 (2000).

[190] A. Fishchuk, J. M. Merritt, and A. van der Avoird (2006), in preparation.

[191] W. M. Fawzy, G. T. Fraser, J. T. Hougen, and A. S. Pine, J. Chem. Phys. **93**, 2992 (1990).

[192] C. M. Western, *Pgopher, a program for simulating rotational structure*, University of Bristol, Bristol, GB.

[193] S. Goyal, D. L. Schutt, and G. Scoles, Phys. Rev. Lett. **69**, 933 (1992), see erratum [242].

[194] K. Nauta and R. E. Miller, J. Chem. Phys. **115**, 10254 (2001).

[195] E. Lee, D. Farrelly, and K. B. Whaley, Phys. Rev. Lett. **83**, 3812 (1999).

[196] A. Viel and K. B. Whaley, J. Chem. Phys. **115**, 10186 (2001).

[197] N. Blinov, X. G. Song, and P. N. Roy, J. Chem. Phys. **120**, 5916 (2004).

[198] K. W. Jucks and R. E. Miller, J. Chem. Phys. **88**, 2196 (1988).

[199] D. S. Anex, E. R. Davidson, C. Douketis, and G. E. Ewing, J. Phys. Chem. **92**, 2913 (1988).

[200] M. Quack and M. A. Suhm, J. Chem. Phys. **95**, 28 (1991).

[201] B. J. Howard, T. R. Dyke, and W. Klemperer, J. Chem. Phys. **81**, 5417 (1984).

[202] B. Kuhn, T. R. Rizzo, D. Luckhaus, M. Quack, and M. A. Suhm, J. Chem. Phys. **111**, 2565 (1999).

[203] G. E. Doublerly and R. E. Miller, J. Phys. Chem. B **107**, 4500 (2003).

[204] D. Blume, M. Lewerenz, F. Huisken, and M. Kaloudis, J. Chem. Phys. **105**, 8666 (1996).

[205] F. Huisken, E. G. Tarakanova, A. A. Vigasin, and G. V. Yukhnevich, Chem. Phys. Lett. **245**, 319 (1995).

[206] F. Huisken, M. Kaloudis, A. Kulcke, C. Laush, and J. M. Lisy, J. Chem. Phys. **103**, 5366 (1995).

[207] D. T. Moore and R. E. Miller, J. Phys. Chem. A **108**, 1930 (2004).

[208] D. T. Moore and R. E. Miller, J. Chem. Phys. **118**, 9629 (2003).

[209] D. T. Moore and R. E. Miller, J. Chem. Phys. **119**, 4713 (2003).

[210] D. T. Moore and R. E. Miller, J. Phys. Chem. A **107**, 10805 (2003).

[211] D. R. Lide, ed., *CRC Handbook of Chemistry and Physics*, vol. 71 (CRC Press, Boca Raton, 1990).

[212] B. R. Strazisar, C. Lin, and H. F. Davis, Science **290**, 958 (2000).

[213] I. W. M. Smith and F. F. Crim, Phys. Chem. Chem. Phys. **4**, 3543 (2002).

[214] P. Zhang, K. Morokuma, and A. M. Wodtke, J. Chem. Phys. **122**, 014106 (2005).

[215] M. Bittererova, H. Ostmark, and T. Brinck, Chem.

Phys. Lett. **347**, 220 (2001).

[216] M. Bittererova, H. Ostmark, and T. Brinck, J. Chem. Phys. **116**, 9740 (2002).

[217] N. Hansen and A. M. Wadtke, J. Phys. Chem. A **107**, 10608 (2003).

[218] F. Cacace, G. de Petris, and A. Troiani, Science **295**, 480 (2002).

[219] E. B. Gordon, L. P. Mezhov-Deglin, O. F. Pugachev, and V. V. Khmelenko, Chem. Phys. Lett. **54**, 282 (1978).

[220] E. B. Gordon, V. V. Khmelenko, A. A. Pelmenev, E. A. Popov, O. F. Pugachev, and A. F. Shestakov, Chem. Phys. **170**, 411 (1993).

[221] R. E. Boltnev, E. B. Gordon, V. V. Khmelenko, I. N. Krushinskaya, M. V. Martynenko, A. A. Pelmenev, E. A. Popov, and A. F. Shestakov, Chem. Phys. **189**, 367 (1994).

[222] E. B. Gordon, V. V. Khmelenko, A. A. Pelmenev, E. A. Popov, and O. F. Pugachev, Chem. Phys. Lett. **155**, 301 (1989).

[223] E. B. Gordon, private communication with R. E. Miller (2000).

[224] R. E. Boltnev et al., in *55th International Symposium on Molecular Spectroscopy* (Ohio State University, Columbus, OH, USA, 2000), WI13, p. 183.

[225] E. A. Popov et al., in *55th International Symposium on Molecular Spectroscopy* (Ohio State University, Columbus, OH, USA, 2000), WI14, p. 183.

[226] E. B. Gordon, Low. Temp. Phys. **30**, 756 (2004).

[227] R. D. Etters, J. John V. Dugan, and R. W. Palmer, The Journal of Chemical Physics **62**, 313 (1975).

[228] I. F. Silvera and J. T. M. Walraven, Phys. Rev. Lett. **44**, 164 (1980).

[229] E. S. Meyer, Z. Zhao, J. C. Mester, and I. F. Silvera, Phys. Rev. B **50**, 9339 (1994).

[230] E. A. Cornell and C. E. Wieman, Rev. Mod. Phys. **74**, 875 (2002).

[231] W. Ketterle, Rev. Mod. Phys. **74**, 1131 (2002).

[232] M. M. Nieto, M. H. Holzscheiter, and T. J. Phillips, J. Opt. B **5**, S547 (2003).

[233] M. G. Kozlov and A. Derevianko, arXiv **physics**, 0602111 (2006), accepted for *Phys. Rev. Lett.*

[234] S. Y. T. van de Meerakker, P. H. M. Smeets, N. Vanhaecke, R. T. Jongma, and G. Meijer, Phys. Rev. Lett. **94**, 023004 (2005).

[235] A. V. Avdeenkov and J. L. Bohn, Phys. Rev. Lett. **90**, 043006 (2003).

[236] A. V. Avdeenkov and J. L. Bohn, Phys. Rev. A **66**, 052718 (2002).

[237] F. Stienkemeier, F. Meier, A. Hagele, H. O. Lutz, E. Schreiber, C. P. Schulz, and I. V. Hertel, Phys. Rev. Lett. **83**, 2320 (1999).

[238] C. P. Schulz, P. Claas, and F. Stienkemeier, Phys. Rev. Lett. **8715**, 153401 (2001).

[239] G. Doppelmann, O. Bunermann, C. P. Schulz, and F. Stienkemeier, Phys. Rev. Lett. **93**, 023402 (2004).

[240] G. Scoles, ed., *Atomic and molecular beam methods*, vol. 1 (Oxford University Press, New York, NY, USA, 1988).

[241] W. B. Zeimen, J. A. Klos, G. C. Groenenboom, and A. van der Avoird, J. Phys. Chem. A **108**, 9319 (2004).

[242] S. Goyal, D. L. Schutt, and G. Scoles, Phys. Rev. Lett. **73**, 2512 (2004).

[243] R. Côté, V. Kharchenko, and M. D. Lukin, Phys. Rev. Lett. **89**, 093001 (2002).

[244] N. Mudrich, O. Bunermann, F. Stienkemeier, O. Dulieu, and M. Weidmüller, Eur. Phys. J. D **31**, 291 (2004).

[245] It is interesting to note that these studies — on systems which are quite similar to the X-HY systems described in section IV A — were performed at the Kaiser Wilhelm-Institut in Berlin-Dahlem: the predecessor of the Fritz Haber-Institut were this review was written.

[246] Commercial atom sources provide so called *clean* atomic beams, but for the purposes of the experiments described here the atom-content is still too low. Initial experiments by ourselves to use microwave discharge sources were not successful due to the necessary low gas flow and pressure, in order not to destroy the helium droplet beam by a gas-jet from the discharge source.

[247] It was recently proposed that similar effects should also be obtainable in atomic Bose-Einstein condensates, where ionic impurities could lead to the formation of *mesoscopic molecular ions* [243].

[248] In a similar approach groups from the field of ultracold atomic physics and helium droplet spectroscopy have successfully collaborated to obtain information on the PES and spectroscopy of mixed alkali dimers [244].